IJMMM International Journal of Minerals, Metallurgy and Materials 矿物冶金与材料学报（英文版）

Surface metal-matrix composites based on AZ91 magnesium alloy via friction stir processing: A review

Hamed Mirzadeh

International Journal of Minerals, Metallurgy and Materials
Volume 30, Number 7, July 2023, Page 1278
https://doi.org/10.1007/s12613-022-2589-y

Invited Review

Surface metal-matrix composites based on AZ91 magnesium alloy via friction stir processing: A review

Hamed Mirzadeh✉

School of Metallurgy and Materials Engineering, College of Engineering, University of Tehran, Tehran, Iran
(Received: 4 October 2022; revised: 30 November 2022; accepted: 20 December 2022)

Abstract: This monograph presents an overview of friction stir processing (FSP) of surface metal-matrix composites (MMCs) using the AZ91 magnesium alloy. The reported results in relation to various reinforcing particles, including silicon carbide (SiC), alumina (Al_2O_3), quartz (SiO_2), boron carbide (B_4C), titanium carbide (TiC), carbon fiber, hydroxyapatite (HA), *in-situ* formed phases, and hybrid reinforcements are summarized. AZ91 composite fabricating methods based on FSP are explained, including groove filling (grooving), drilled hole filling, sandwich method, stir casting followed by FSP, and formation of *in-situ* particles. The effects of introducing second-phase particles and FSP process parameters (e.g., tool rotation rate, traverse speed, and the number of passes) on the microstructural modification, grain refinement, homogeneity in the distribution of particles, inhibition of grain growth, mechanical properties, strength–ductility trade-off, wear/tribological behavior, and corrosion resistance are discussed. Finally, useful suggestions for future work are proposed, including focusing on the superplasticity and superplastic forming, metal additive manufacturing processes based on friction stir engineering (such as additive friction stir deposition), direct FSP, stationary shoulder FSP, correlation of the dynamic recrystallization (DRX) grain size with the Zener–Hollomon parameter similar to hot deformation studies, process parameters (such as the particle volume fraction and external cooling), and common reinforcing phases such as zirconia (ZrO_2) and carbon nanotubes (CNTs).

Keywords: surface composites; magnesium alloys; friction stir processing; severe plastic deformation; thermomechanical processing

1. Introduction

Magnesium alloys and composites are used in various industries owing to their good specific strength, high damping capacity, good castability, and biodegradability [1–4]. They are considered to be the ultimate choice of lightweight metallic structural materials [5–6]. However, polycrystalline Mg is characterized by poor ductility due to the presence of a hexagonal close-packed (hcp) crystal structure with few slip systems. Moreover, the relatively lower strength of Mg alloys compared to other competing alloys is another major obstacle to their utilization in many potential applications [7]. These shortcomings can be relieved by alloying [8–9], heat treatment [10–11], elevated temperature thermomechanical processing [12–13], severe plastic deformation (SPD) [14], and introduction of reinforcement particles (Mg-based metal-matrix composites (MMCs)) [15–16].

Among SPD techniques, friction stir processing (FSP), which is based on the principles of friction stir welding (FSW), is a viable technique for material processing [17–18]. FSP is applied by pushing a rotating tool into the surface of the workpiece, followed by its translational movement. This nonconsumable tool consists of a cylindrical shoulder and a projecting concentrically located pin (probe). During FSP, the material is locally softened due to the heat generated by the friction between the tool and workpiece, as well as through auxiliary adiabatic heating due to plastic deformation during the flow of the material [19]. FSP is normally used for microstructural enhancement (e.g., grain refinement by dynamic recrystallization [20–21] and altering the amount, morphology, and distribution of particles [22]), improvement of various properties (e.g., mechanical properties [23] and superplasticity [24]), and processing of composites [25]. FSP is an efficient method for processing surface composites [26], whereby the second-phase particles can be introduced to the surface via narrow grooves or drilled holes before FSP [27], as schematically shown in Fig. 1. After filling the grooves or holes with particles, an optional closing (covering) step can be carried out using a pinless FSP tool to avoid the escape of the particles during the subsequent main FSP step [28]. As shown in Fig. 1, from the stir zone (SZ, or nugget zone, NZ) to base metal (BM), a thermomechanically affected zone (TMAZ) and a heat-affected zone (HAZ) will develop [29]. The primary processing parameters include tool geometry, tool rotation rate (ω, r/min), and traverse/advancing/welding speed (v, mm/min) [30]. A higher ω or lower v normally leads to a higher temperature [31]. The grain size can be refined by decreasing ω at constant v or by

✉ Corresponding author: Hamed Mirzadeh E-mail: hmirzadeh@ut.ac.ir

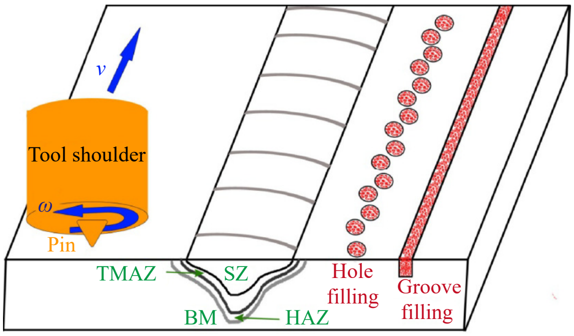

Fig. 1. Schematic representation of the surface composite fabrication by FSP.

increasing *v* at constant *ω* [32]. Anyway, adequate heating is always required to produce a defect-free nugget with a refined microstructure [33].

Another FSP-based composite fabrication method for Mg alloys is direct friction stir processing (DFSP) [34–36]. In the DFSP process, the secondary phase is *in-situ* introduced to the enclosed space between the shoulder of a pinless tool and the base metal through a hole provided within the FSP tool, followed by pressing them into the workpiece as the rotating tool advances along them just like a planter (Fig. 2) [34]. This method has been successfully applied to AZ31/SiC composite [34]. Moreover, there are some promising and innovative modifications, such as friction stir welding with a pulse current [18]. Furthermore, the potential to use the stationary shoulder tool in FSP as a novel low-heat input tooling system for Mg alloys has been extensively studied by Patel *et al.* [37–39]. As shown in Fig. 3, a rotating tool (consisting of a probe with a small or no shoulder) is housed within a nonrotational shoulder (stationary shoulder)—the tool slides over the joint line during processing to eliminate or minimize the heat generated by the shoulder [39]. As a result, lower and more focused heat will be generated through the thickness [37]. Due to the stationary action of the shoulder, this process generates a smooth surface [40] with a small amount of flash onto the surface [41] and develops uniform grain refinement and, consequently, homogeneous mechanical properties throughout the thickness. In other words, the small temperature gradient across the thickness of the SZ in this process leads to the homogenization of the magnesium alloy microstructure [38].

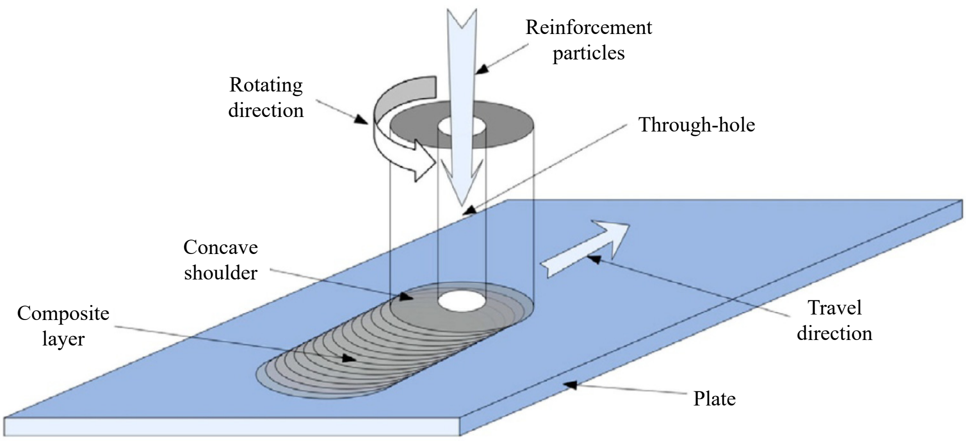

Fig. 2. Schematic representation of direct friction stir processing [34]. Reprinted from *Mater. Des.*, Vol. 59, Y.X. Huang, T.H. Wang, W.Q. Guo, L. Wan, and S.X. Lv, Microstructure and surface mechanical property of AZ31 Mg/SiC$_p$ surface composite fabricated by direct friction stir processing, 274-278, Copyright 2014, with permission from Elsevier.

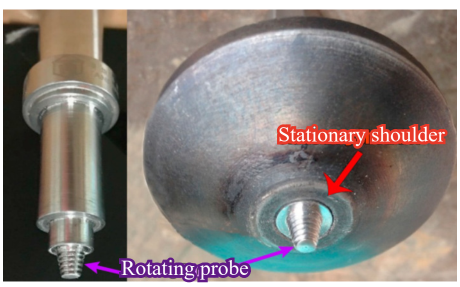

Fig. 3. Stationary shoulder tooling system [39].

The most widely used Mg alloys are based on the AZ series (Mg–Al–Zn) [42], among which the AZ91 (Mg–9Al–1Zn, wt%) is one of the famous alloys [43]. The presence of the eutectic structure (α-Mg/$Mg_{17}Al_{12}$) deteriorates the mechanical and functional properties of the AZ series Mg alloys [44]. The dissolution of the $Mg_{17}Al_{12}$ phase during elevated temperature processing increases the Al content of the matrix [45], which might result in a major solid solution strengthening effect [46]. Moreover, the fragmentation and dispersion of $Mg_{17}Al_{12}$ particles during processing reduce their deleterious effects. FSP can simultaneously apply SPD and elevated temperature thermomechanical processing in the solid state [46–47]. Accordingly, recrystallization processes can refine the microstructure and enhance the material properties; while dissolution, fragmentation, and dispersion of particles can effectively amend the adverse effects of intergranular eutectics in AZ91 alloy [48]. Accordingly, FSP can be considered a viable processing method for AZ91 alloy [49]. The processing of fine-grained and high-performance AZ91 composites by FSP is fairly easy. Accordingly, the present overview article is dedicated to summarizing reported works on the FSP of AZ91 composites and indicating key suggestions for future works.

2. AZ91 composites fabricated by FSP

2.1. AZ91–SiC composites

AZ91–SiC (silicon carbide) composites are among the most widely investigated ones. Asadi *et al.* [50] fabricated composite layers on the surface of as-cast AZ91 Mg alloy using nanosized (30 nm) and micron-sized (5 µm) SiC particles (using groove filling and covering method). With the application of FSP, a fine microstructure was obtained with the dissolution of the eutectic $Mg_{17}Al_{12}$ phase in the SZ for as-cast AZ91 Mg alloy and composites, as shown in Fig. 4(a). The addition of SiC led to more intense grain refinement and enhancement of hardness, where these effects were more pronounced for nanosized SiC particles compared to the micron-sized SiC particles, as shown in Fig. 4(b) and (c). Moreover, lower ω and/or higher v led to a finer grain size and greater hardness, as shown in Fig. 4(b) and (c) [50]. The dependence of the grain size on the FSP parameters has also been reported for AZ91/SiC surface composite (using hole filling or multichamber technology) by Iwaszko *et al.* [51]. In another study, Asadi *et al.* [52] showed that the repetition of the FSP passes leads to more pronounced grain refinement and en-

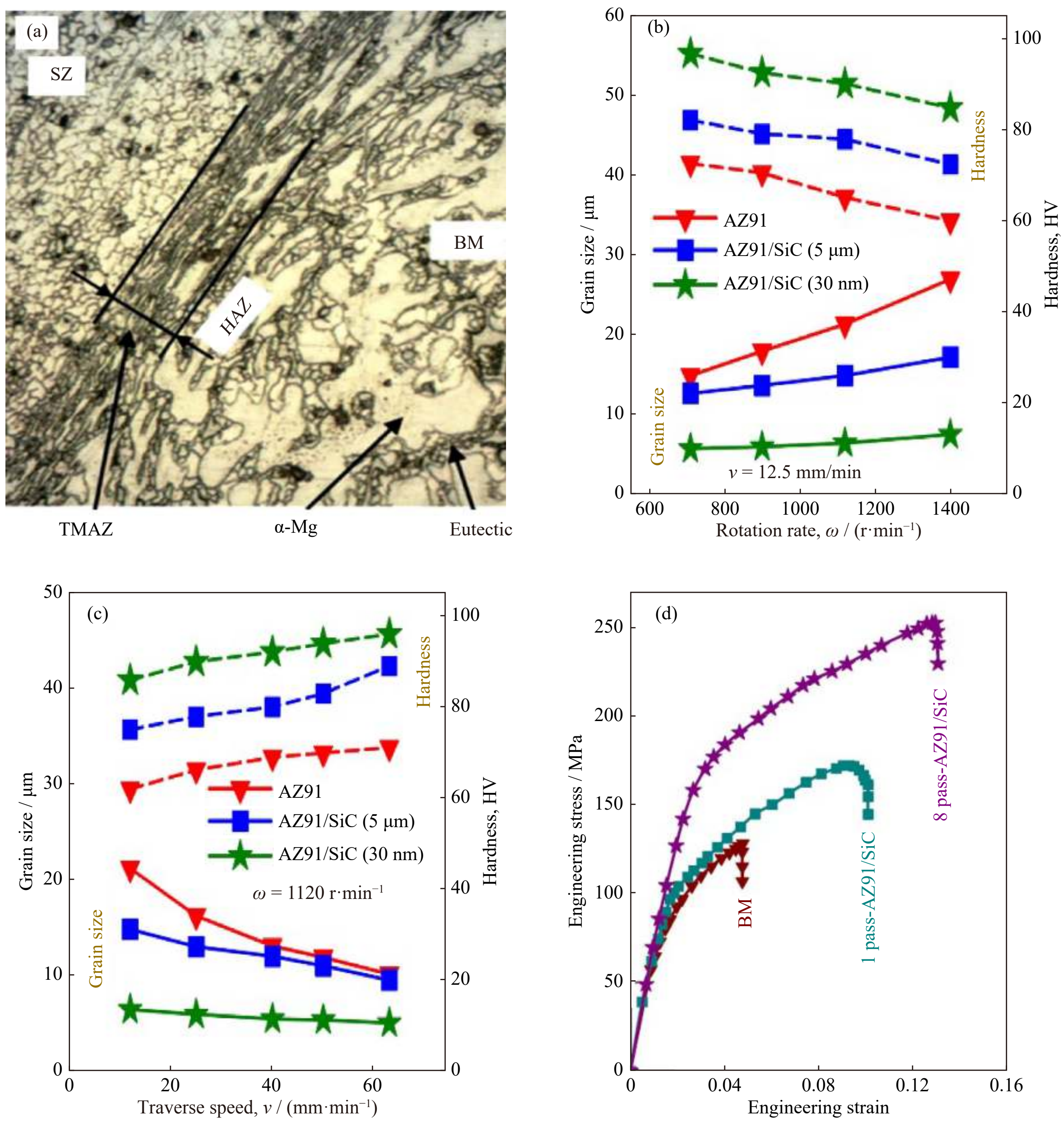

Fig. 4. (a) Representative FSP microstructure, (b, c) dependence of stir zone grain size and hardness on the FSP parameters, and (d) tensile stress–strain curves of FSP AZ91/SiC surface composites (the curves are redrawn) [50,52]. (a–c) Adapted by permission from Springer Nature: *J. Mater. Eng. Perform.*, Effects of SiC particle size and process parameters on the microstructure and hardness of AZ91/SiC composite layer fabricated by FSP, P. Asadi, M.K.B. Givi, K. Abrinia, M. Taherishargh, and R. Salekrostam, Copyright 2011; (d) adapted by permission from Springer Nature: *Metall. Mater. Trans. A*, Experimental investigation of magnesium-base nanocomposite produced by friction stir processing: Effects of particle types and number of friction stir processing passes, P. Asadi, G. Faraji, A. Masoumi, and M.K.B. Givi, Copyright 2011.

hanced mechanical properties (Fig. 4(d)), a finding that was confirmed by Dadaei *et al.* [53] who used the groove filling and covering method.

Bagheri *et al.* [54] proposed friction stir vibration processing (FSVP) as an improved and efficient FSP method for the processing of magnesium alloys and composites. During the process, the workpiece is vibrated in a direction that is normal to the tool translational direction, as shown in Fig. 5(a). The FSP and FSVP techniques were used to process AZ91/SiC surface composites using the groove filling and covering method. A more homogeneous distribution of SiC particles was observed for FSVP compared to FSP. In the FSVP process, workpiece vibration resulted in higher plastic strain in the material, hence promoting dynamic recrystallization. Consequently, finer grains were developed when using FSVP than when using FSP (Fig. 5(b)), indicating that FSVP results in better mechanical properties, as depicted in Fig. 5(c).

Eq. (1) can be used to correlate the dynamically recrystallized grain size (d) with the Zener–Hollomon parameter (Z, Eq. (2)), where A and B are constants, and R is the gas constant. The deformation activation energy (Q) is normally considered to be the activation energy for lattice self-diffusion [55–57]. The deformation temperature (T) and strain rate ($\dot{\varepsilon}$) during FSP can be estimated by Eq. (3) [58–59] and Eq. (4) [59–60], where T_m is the absolute melting point of the material; K and α are constants; R_{nugget} and D_{nugget} are the effective (or average) radius and depth of the dynamically recrystallized zone [58–62]. These formulas might also be applied when discussing the effects of modification in the FSP processes. For instance, Bagheri *et al.* [63] have noted that R_{nugget} for the FSVP (Fig. 5(a)) is larger than that for FSP (due to vibration). Accordingly, the strain rate and the Z parameter are higher in FSVP, which is favorable for grain refinement.

$$d = AZ^{-B} \quad (1)$$

$$Z = \dot{\varepsilon}\exp\left(\frac{Q}{RT}\right) \quad (2)$$

$$\frac{T}{T_m} \approx K\left(\frac{\omega^2}{v\times 10^4}\right)^{\alpha},\ 0.04 \le \alpha \le 0.06,\ 0.65 \le K \le 0.75 \quad (3)$$

$$\dot{\varepsilon} \approx \pi\omega\frac{R_{nugget}}{D_{nugget}} \quad (4)$$

Another modification for grain refinement is the FSP with external cooling [64–66], which is related to temperature modification and is used to inhibit extensive grain growth and dissolution of precipitates in and around the stirred zone [19]. As shown by Patel *et al.* [67], the backing plate is also

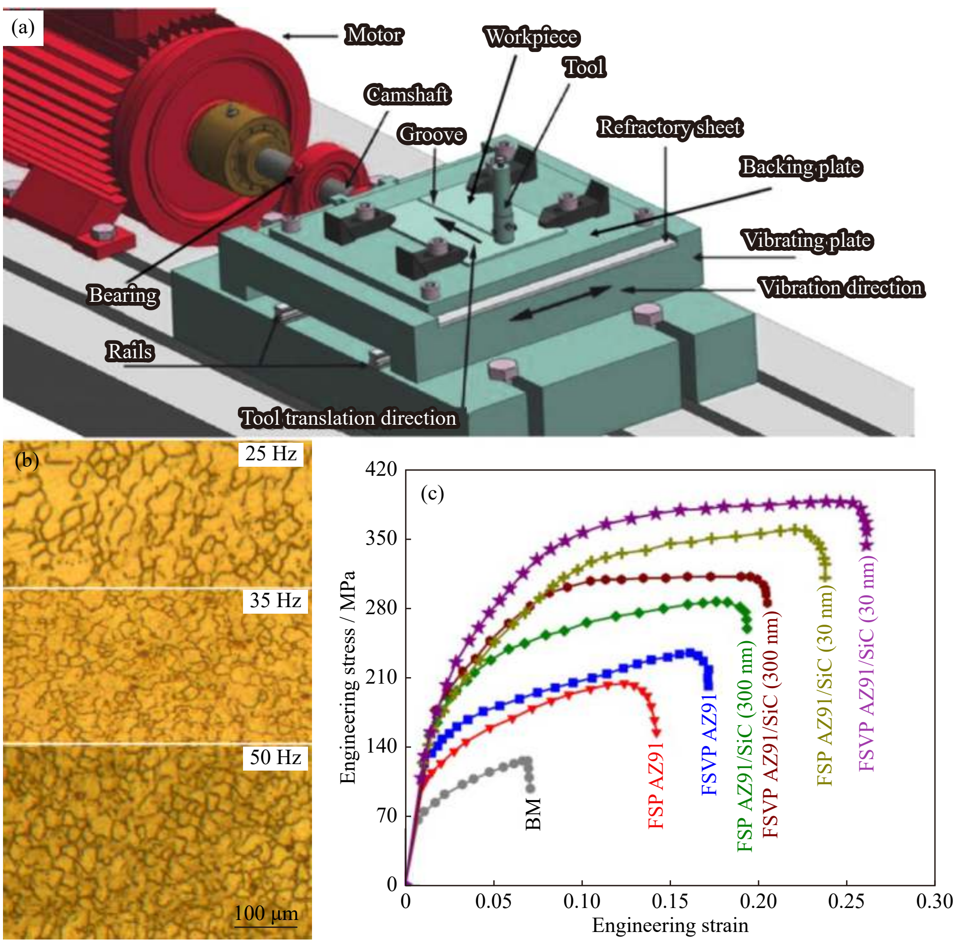

Fig. 5. (a) Schematic representation of FSVP, (b) the effect of vibration frequency on FSVP microstructure, and (c) tensile stress–strain curves of AZ91/SiC surface composites (the curves are redrawn) [54]. Reprinted from *Trans. Nonferrous Met. Soc. China*, Vol. 30, B. Bagheri, M. Abbasi, A. Abdollahzadeh, and S.E. Mirsalehi, Effect of second-phase particle size and presence of vibration on AZ91/SiC surface composite layer produced by FSP, 905-916, Copyright 2020, with permission from Elsevier.

important—a copper backing plate was found to be more effective than a steel backing plate for grain refinement of Mg alloys.

Similar to the results of Asadi *et al.* [50], Bagheri *et al.* [54] also found finer SiC particles to be more conducive to obtaining better mechanical properties. Accordingly, high-performance AZ91 composites can be processed through the addition of nanosized particles combined with FSVP. The favorable effect of increasing vibration frequency on grain refinement can be seen in Fig. 5(b) [54].

Due to the dissolution of the β-$Mg_{17}Al_{12}$ phase during FSP, the AZ91 alloy might have the next best aging response after FSP. Accordingly, Shang *et al.* [68] examined the aging behavior of FSP AZ91 alloy and the AZ91/SiC composite (50 nm, based on the hole-filling method). With the addition of nanosized SiC particles [69], a more intense grain refinement after FSP was observed (Fig. 6(a)). However, while a higher hardness level was obtained, the age hardening efficiency became inferior for AZ91/SiC composite compared to AZ91 alloy (Fig. 6(b)) [68] .

The discontinuous precipitation of the β-phase that dominated the FSP AZ91 alloy was significantly restricted in the composite, and the nanosized SiC particles promoted continuous precipitation of the β-phase. While there was no significant difference in the amounts of precipitated β-phase between the FSP AZ91D and AZ91/SiC (the formation of precipitates during aging can be seen in the X-ray diffraction (XRD) patterns of Fig. 6(c)), the different precipitation behaviors and different strengthening mechanisms were found to be responsible for the difference in aging responses, for which the particle size and distribution might play decisive roles [68].

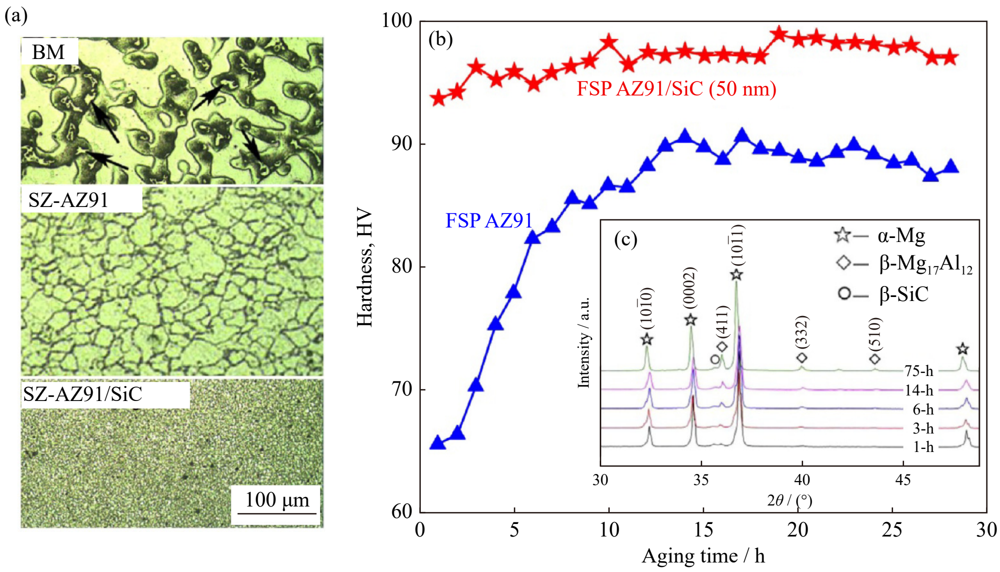

Fig. 6. (a) Representative optical micrographs (the arrows denote the β-$Mg_{17}Al_{12}$ phase), (b) aging responses of AZ91 alloy and AZ91/SiC composite at 180°C, and (c) XRD patterns of AZ91/SiC composite at different aging times at 180°C [68]. Reprinted from *J. Alloys Compd.*, Vol. 797, J.L. Shang, L.M. Ke, F.C. Liu, F.Y. Lv, and L. Xing, Aging behavior of nano SiC particles reinforced AZ91D composite fabricated via friction stir processing, 1240-1248, Copyright 2019, with permission from Elsevier.

Chen *et al.* [70] investigated the effects of FSP and SiC addition (using the groove filling method) on thixoformed AZ91 alloy. A uniform distribution of SiC particles was obtained via FSP (Fig. 7(a)). The alloy with a composite surface showed higher hardness and wear resistance and lower friction coefficient as compared to the permanent mold cast and the thixoformed alloy without a composite surface, as shown in Fig. 7(b). The composite surface showed good tribological properties due to the strengthening roles played by the particles.

Lee *et al.* [71] also showed the enhancement of wear resistance in AZ91/SiC composites through FSP processing. In another study, Abbasi *et al.* [72] reported that by applying more FSP passes during the processing of AZ91/SiC surface composite, the mechanical properties improved, corrosion resistance increased, and the wear rate decreased. More recently, Abdollahzadeh *et al.* [73] reported the improvement of wear and corrosion resistance of AZ91/SiC composite layer processed by FSVP compared to FSP.

2.2. AZ91–Al_2O_3 composites

Faraji *et al.* [74–75] fabricated composite layers on the surface of as-cast AZ91 Mg alloy using nanosized Al_2O_3 (alumina) particles (30 nm, using the groove filling method). Fig. 8(a) shows the typical surface appearance of processed composites, in which defects such as voids and cracks cannot be observed [75]. By increasing v at a constant ω of 900 r/min, the grain size was refined, and the hardness increased. Accordingly, the optimum condition for producing a sound and fine-grained surface layer was characterized as ω = 900 r/min and v = 80 mm/min. More recently, Ahmadkhaniha *et al.* [76] processed AZ91/Al_2O_3 surface composites using nanosized Al_2O_3 particles (50 nm, using the groove filling and covering method), and the optimum values of ω = 800

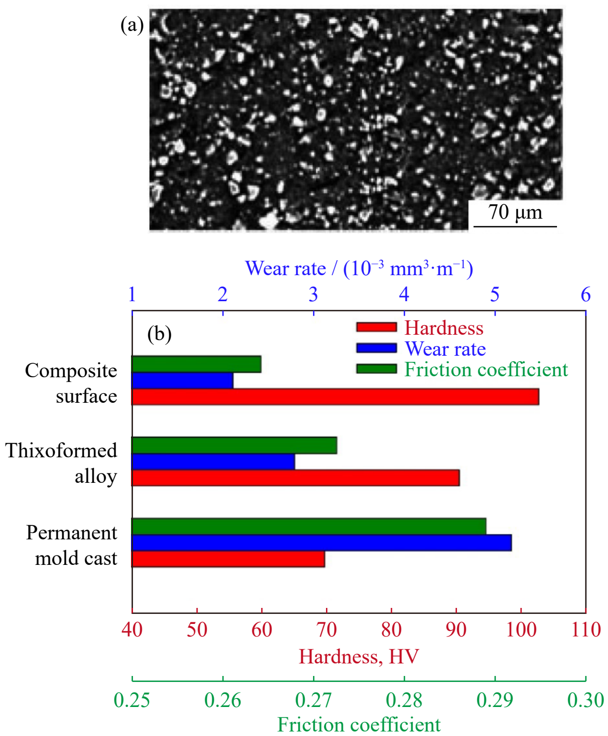

Fig. 7. (a) Scanning electron microscopy (SEM) image of the AZ91/SiC surface composite processed by FSP and (b) the comparison of its properties with AZ91 alloy processed by other techniques [70]. Adapted by permission from Springer Nature: *J. Wuhan Univ. Technol. Mater. Sci. Ed.*, Friction stir processing of thixoformed AZ91D magnesium alloy and fabrication of surface composite reinforced by SiC$_p$s, T.C. Chen, Z.M. Zhu, Y. Ma, Y.D. Li, and Y. Hao, Copyright 2010.

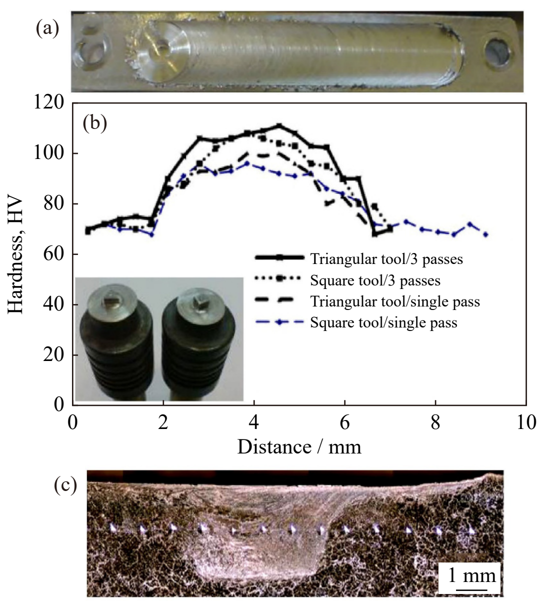

Fig. 8. (a) Top face of the specimen produced by FSP; (b) effect of tool geometry and number of passes on hardness profile (inset shows the used FSP tools); (c) image of the processed region (indicating the indentation locations) [75]. Reprinted by permission from Springer Nature: *J. Mater. Eng. Perform.*, Effect of process parameters on microstructure and micro-hardness of AZ91/Al$_2$O$_3$ surface composite produced by FSP, G. Faraji, O. Dastani, and S.A.A. Mousavi, Copyright 2011.

r/min and v = 40 mm/min were suggested for obtaining the highest hardness and wear resistance. The authors also proposed the Hall–Petch-type formula that relates hardness (H, HV) to grain size (d, μm), i.e., $H = \frac{55.88}{\sqrt{d}} + 67.453$. Faraji *et al.* [75] also investigated the effects of Al_2O_3 particle size, tool geometry, and repetition of FSP passes. It was found that decreasing the size of Al_2O_3 particles leads to more intense grain refinement and an increase in hardness. Moreover, a higher number of FSP passes using triangular tool geometry can produce a harder surface composite, as shown in Fig. 8(b) and (c). In fact, the triangular tool was more effective compared to the square tool. Increasing the number of passes also enhanced the homogeneity and particle distribution and resulted in a more refined grain size distribution [75].

The AZ91/Al_2O_3 and AZ91/SiC surface composites processed by FSP have been compared by Asadi *et al.* [52], Dadaei *et al.* [53], and Abbasi *et al.* [72]. These studies generally demonstrate that the microstructure of the composite layer created by SiC particles is characterized by finer grains, as well as higher hardness, strength, elongation, corrosion resistance, and wear resistance compared to the composite layer by Al_2O_3 particles. Polarization curves comparing corrosion resistance between AZ91/Al_2O_3 and AZ91/SiC surface composites are shown in Fig. 9 [72], which depict that the AZ91/SiC surface composite has a lower corrosion current density i_{corr} (as can be obtained based on the Tafel extrapolation method [77]) and more positive corrosion potential E_{corr}. By investigating the strength/weight ratios of as-cast and FSP AZ91 alloys, as well as AZ91/Al_2O_3 and AZ91/SiC composites, Dadaei *et al.* [53] proved the positive impact of FSP and significant enhancements for composites at higher FSP passes. Therefore, it can be deduced that the desirable

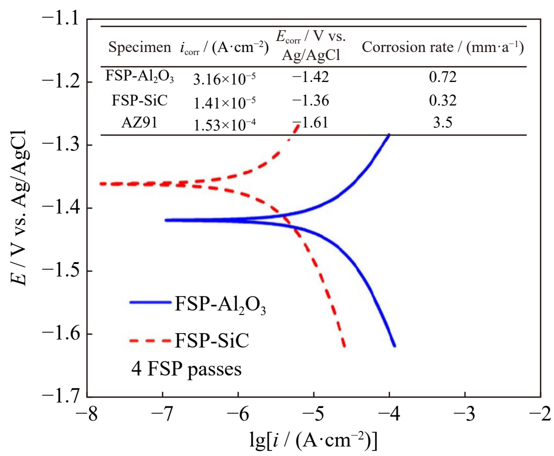

Fig. 9. Polarization curves for FSP AZ91 alloys and composites (the inserted table shows the potentials, current densities, and corrosion rates obtained by Tafel extrapolarization analyses of both the FSPed specimens and the original AZ91 alloy) [72]. Reprinted by permission from Springer Nature: *Int. J. Adv. Manuf. Technol.*, The effect of FSP on mechanical, tribological, and corrosion behavior of composite layer developed on magnesium AZ91 alloy surface, M. Abbasi, B. Bagheri, M. Dadaei, H.R. Omidvar, and M. Rezaei, Copyright 2015.

effects of particle addition can be achieved after several FSP passes.

2.3. AZ91–SiO_2 composites

Vignesh *et al.* [78] fabricated a composite layer on the surface of AZ91 Mg alloy using nanosized SiO_2 (quartz) particles (15 nm, using groove filling and covering method). Low tool rotation rate and traverse speed resulted in poor material flow. Composites processed at low tool rotation rates and high tool traverse speed had scalloped surfaces and wormholes. A high tool rotation rate and high tool traverse speed resulted in turbulent material flow, leading to a lack of fusion and root flow defects. However, a high tool rotation rate and low tool traverse speed led to a defect-free processed region with a fine dispersion of the reinforcements in the matrix. Accordingly, the process window for the AZ91/SiO_2 composite was constructed, as shown in Fig. 10(a).

The simulation of temperature change during FSP of AZ91 alloy was performed based on the Comsol Multiphysics 5.0 software; an example is shown in Fig. 10(b) [78], revealing a significant increase in the temperature during FSP. Based on the simulation results, it was found that the peak temperature associated with FSP increases with an increase in tool rotation rate or a decrease in tool traverse speed [78]. In this context, Khayyamin *et al.* [79] reported more intense grain refinement and increased hardness for the AZ91/SiO_2 composite (using the groove filling and covering method) by increasing the traverse speed at a constant tool rotation rate.

The hardness profile along the transverse section is shown in Fig. 10(c) [78]. The figure reveals a much higher hardness in the SZ compared to the hardness of the base metal. This enhancement can be attributed to grain refinement as well as to the presence of a fine dispersion of β-$Mg_{17}Al_{12}$ phase and nanophase SiO_2 particles. The fine dispersion of SiO_2 accentuated the refinement of the matrix through its effects on the nucleation of recrystallization and inhibition of grain growth [80–81]. The corrosion test results revealed the formation of an adherent layer of calcium hydroxyapatite and calcium–magnesium phosphate in simulated body fluids, which reduced the corrosion rate for bioimplant applications [78].

Khayyamin *et al.* [79] also fabricated composite layers on the surface of the AZ91 alloy using nanosized SiO_2 particles (10 nm). FSP led to the refinement of the matrix grains. Increasing the traverse speed at ω = 1250 r/min resulted in greater grain refinement and enhanced tensile properties, as shown in Fig. 11(a). Moreover, by increasing the number of passes, better uniformity in the particle distribution and finer grain sizes were obtained, which led to the further improvement of the mechanical properties (Fig. 11(b)). In this regard, the dissolution/dispersion of the β-$Mg_{17}Al_{12}$ phase and the closure of casting defects have also been indicated [79].

In fact, controlling the distribution of reinforcing particles plays a key role in the performance of the fabricated composites [82–83]. An ideal metallic composite should have a homogeneous distribution of particulates and constant interparticle distance. The resultant composite microstructure should approach this condition in order to exhibit improved mechanical properties [84]. The improvement of particle distribution enhances the material flow and prevents early fracture, thereby improving the tensile ductility of the composite. Conversely, cluster formation might lead to poor tensile strength and elongation [84]. The homogeneous distribution is a result of the rotating tool's effective stirring action [84] as well as the extrusion of the plasticized material due to the movement of the tool [85], which are primarily influenced by the major process parameters, including tool rotational speed and traverse speed [84,86–87]. Traverse speed affects both frictional heat and mechanical stirring simultaneously, leading to poor particle dispersion at increased traverse speed [84,88]. Moreover, there is evidence that increasing the rotational rate leads to improved particle distribution [28,88]. Furthermore, increasing the number of FSP passes can promote the uniform distribution of particles [28,84,88]. In other words, the repeated stirring action and the plastic flow of the material tend to reduce particle agglomeration [84]. Although this is the most effective strategy, a corresponding increase in production costs should also be taken into account [28].

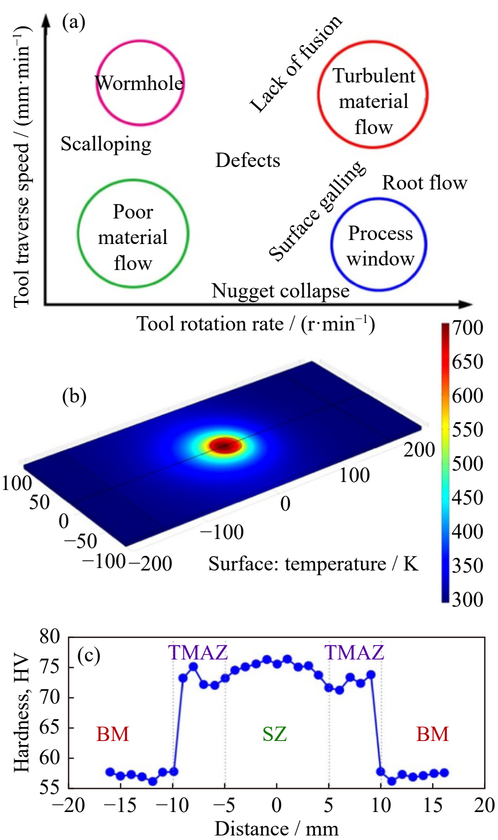

Fig. 10. (a) FSP process window for synthesizing AZ91/SiO_2 composite, (b) simulation of the thermal phenomenon during FSP for ω = 600 r/min and v = 40 mm/min, and (c) hardness profile along the transverse section for ω = 900 r/min and v = 20 mm/min [78]. Reprinted by permission from Springer Nature: *Silicon*, Synthesis and characterization of magnesium alloy surface composite (AZ91D–SiO_2) by friction stir processing for bioimplants, R.V. Vignesh, R. Padmanaban, and M. Govindaraju, Copyright 2020.

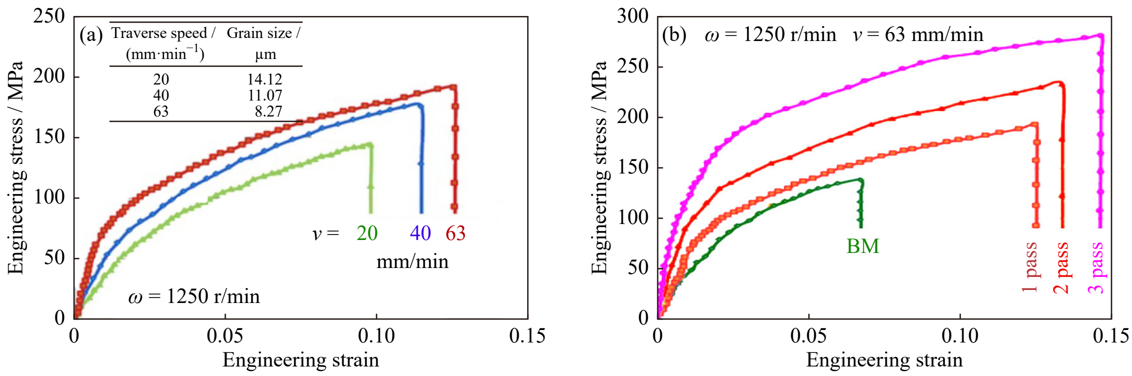

Fig. 11. Tensile stress–strain curves of AZ91/SiO_2 surface composites for (a) various *v* values at *ω* = 1250 r/min (the inserted table shows effect of the traverse speed on the final grain size in the SZ of the specimens) and (b) various passes at *ω* = 1250 r/min at *v* = 63 mm/min [79]. Reprinted from *Mater. Sci. Eng. A*, Vol. 559, D. Khayyamin, A. Mostafapour, and R. Keshmiri, The effect of process parameters on microstructural characteristics of AZ91/SiO_2 composite fabricated by FSP, 217-221, Copyright 2013, with permission from Elsevier.

The effect of the FSP tool might be significant [89]. For instance, a profound effect has been observed on the particle size distribution uniformity when using a tool with a square pin than when using one with a circular pin [28]. Moreover, changing the direction of tool rotation during multipass FSP might also lead to better grain refinement and more homogeneous particle distribution [90]. Furthermore, novel FSP variants such as the bobbin tool FSP (BTFSP) can be used for fabricating two-side composites on the top and bottom sides of the workpiece, as shown in Fig. 12, where good uniformity in the particle distribution can be achieved [91]. A low plunge depth level might lead to insufficient heat generation and cavity formation toward the SZ center. On the other hand, high levels of plunge depth result in the ejection of reinforcement particles and even the sticking of material to the tool shoulder. Thus, an optimal plunge depth is needed in developing defect-free surface composites [92].

The particle volume fraction (*f*) can be adjusted based on the shape/size of grooves or the depth/number of holes. The microstructure and properties of the composite are dependent on *f*, where an example is shown in Fig. 13 for FSP AZ31/Ti composite [87]. For grove filling, *f* can be estimated by Eq. (5) [93]. It is noteworthy that it is difficult to control the number of particles that can be introduced into the surface, and there may be a nonuniform distribution of the particles in the thickness direction [28]. Another concern is the severe tool wear when FSP is used with composites with a high *f*, as discussed by Avettand-Fènoël and Simar [30]. Generally, an increase in the particulate content might raise the difficulty of plasticization, which can adversely affect particle distribution homogeneity [84]. On the other hand, an increase in the particulate content can further reduce the ductility of the intrinsically brittle Mg matrix. However, grain refinement of α-Mg might lead to the activation of secondary slip systems, which is advantageous [94]. Using deformable particles such as Ti alloys as reinforcing particles can help maintain ductility [86–87].

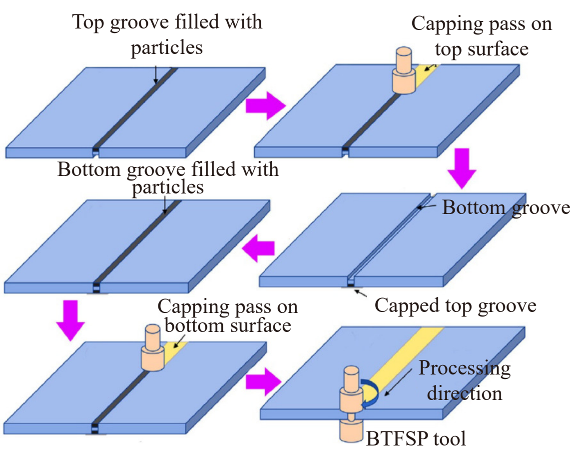

Fig. 12. Schematic diagram of the steps followed for fabricating double-side composite using bobbin tool friction stir processing [91].

$$\begin{cases} f = A_G/A'_P \\ A_G = \text{area of groove} = \text{groove width} \times \text{groove depth} \\ A'_P = \text{projected area of pin} = \text{pin diameter} \times \text{pin length} \end{cases} \tag{5}$$

2.4. AZ91–B_4C composites

Patle *et al.* [95] fabricated composite layers on the surface of as-cast AZ91 Mg alloy using micron-sized B_4C (boron carbide) particles (10–15 μm, using groove filling and covering method). A defect-free processed region was obtained for *ω* = 1400 r/min and *v* = 22 mm/min. As shown in Fig. 14, the surface composite showed higher hardness compared to the base metal, which was attributed to the dispersed B_4C particles and microstructural refinement in the SZ. Moreover, the processed surface composite showed a lower wear rate. The wear mechanisms were found to be dependent on the sliding velocity. For a sliding velocity of 0.06 m/s, the predominant wear mechanisms were abrasive and severe adhesive wear, along with some degree of oxidative wear; whereas, for a sliding velocity of 0.12 m/s, delamination and oxidative wear were the predominant ones, along with some abrasive and mild adhesive wear. Singh *et al.* [96] also fabricated AZ91/B_4C surface composite by FSP (*ω* = 900 r/min and *v* = 45 mm/min, using hole filling method) and reported enhancement of wear resistance based on the wear tests performed by the pin-on-disk apparatus.

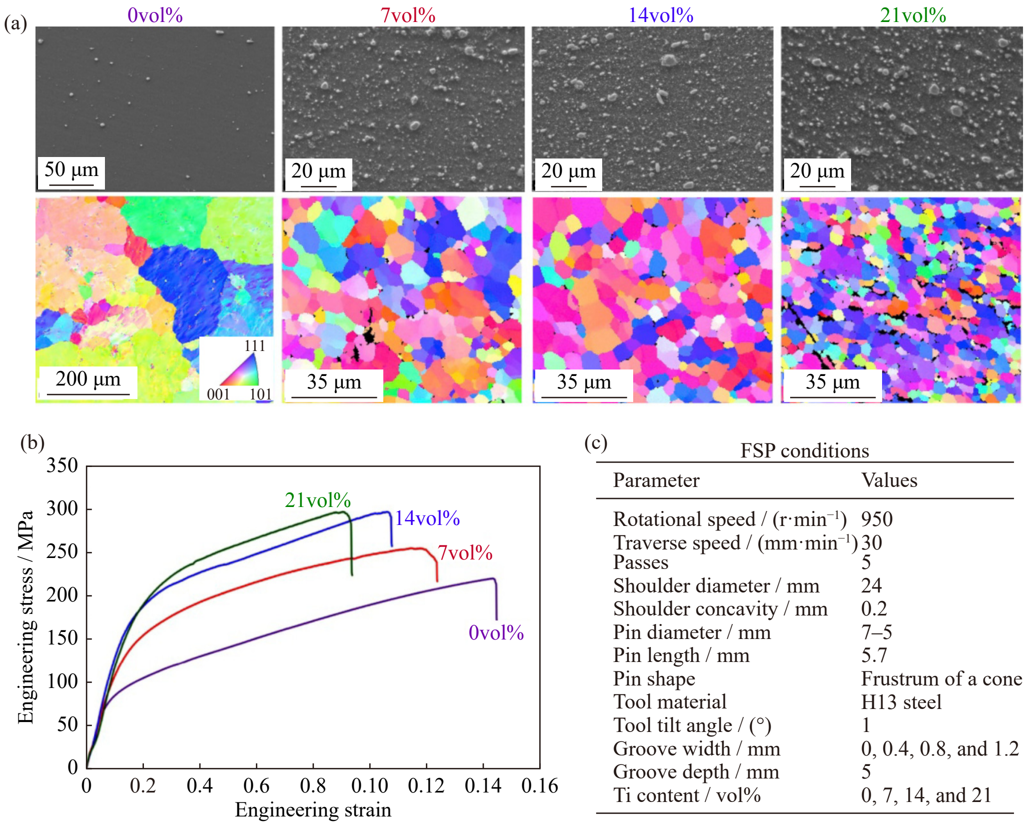

FSP conditions

Parameter	Values
Rotational speed / (r·min^{-1})	950
Traverse speed / (mm·min^{-1})	30
Passes	5
Shoulder diameter / mm	24
Shoulder concavity / mm	0.2
Pin diameter / mm	7–5
Pin length / mm	5.7
Pin shape	Frustrum of a cone
Tool material	H13 steel
Tool tilt angle / (°)	1
Groove width / mm	0, 0.4, 0.8, and 1.2
Groove depth / mm	5
Ti content / vol%	0, 7, 14, and 21

Fig. 13. (a) SEM images and electron backscattered diffraction (EBSD) maps, (b) tensile stress–strain curves of Ti-reinforced AZ31 composites processed by FSP, and (c) the FSP parameters used for processing [87]. Reprinted from *Mater. Sci. Eng. A*, Vol. 772, I. Dinaharan, S. Zhang, G.Q. Chen, and Q.Y. Shi, Titanium particulate reinforced AZ31 magnesium matrix composites with improved ductility prepared using friction stir processing, 138793, Copyright 2020, with permission from Elsevier.

2.5. AZ91–TiC composites

Vijayan *et al.* [97] processed AZ91/TiC (titanium carbide) surface composite using micron-sized TiC particles (4 μm, using groove filling and covering method). Defect-free surface composite with equiaxed recrystallized grains in the nugget zone with homogeneously distributed TiC particles was obtained using $\omega = 1000$ r/min, $v = 30$ mm/min, and an 8 kN axial load. The surface composite had a peak hardness of almost twice that of the base metal. Accordingly, the pin-on-disk wear test revealed the superiority of wear resistance of the surface composite compared to the base metal, as shown in Fig. 15.

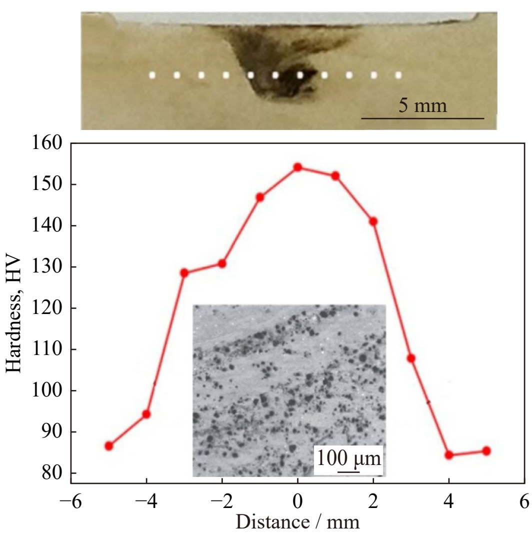

Fig. 14. Hardness profile along the transverse section and a representative SEM image from the processed area of FSP AZ91/B_4C composite [95].

Sahoo *et al.* [98] processed AZ91/TiC–TiB_2 *in-situ* hybrid composite by stir casting, whereby the TiC–TiB_2 reinforcements were formed *in-situ* [99] via the addition of ball-

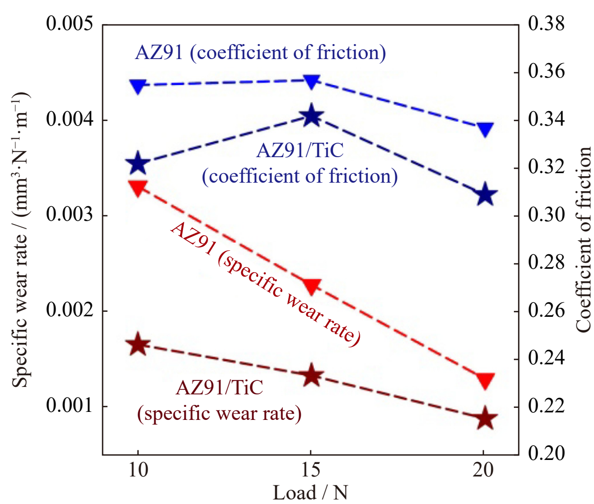

Fig. 15. Specific wear rate and coefficient of friction versus load for FSP AZ91/TiC composite compared to those obtained for AZ91 alloy [97].

milled Ti–B_4C powder. The as-cast *in-situ* composite was then subjected to FSP for microstructural refinement. From the EBSD maps shown in Fig. 16 for AZ91 and AZ91/TiC–TiB_2, FSP led to remarkable grain refinement. The SEM images in Fig. 16 also show that applying FSP and its repetition (pass 2) resulted in the formation of a more uniform microstructure due to the elimination of the continuous network of the β-$Mg_{17}Al_{12}$ phase of the as-cast state. The presence of the *in-situ* TiC–TiB_2 reinforcement particles in the AZ91/TiC–TiB_2 composite can effectively result in grain growth resistance at the grain boundaries; hence a finer grain size has been achieved for the AZ91/TiC–TiB_2 composite.

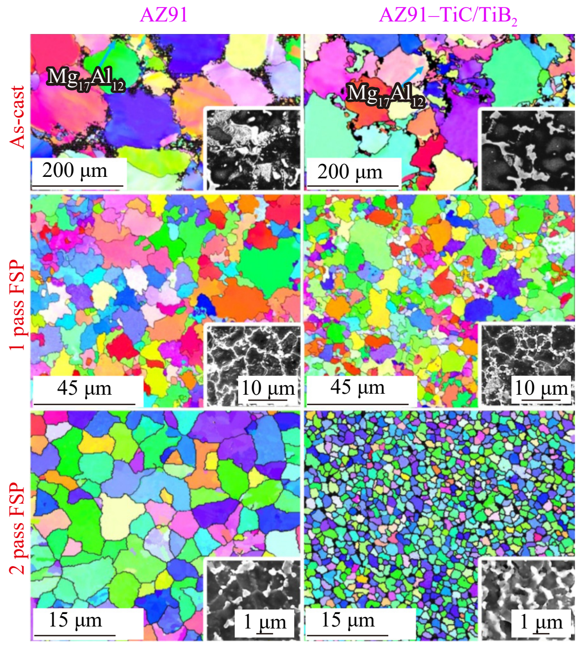

Fig. 16. EBSD maps and SEM images (insets) of as-cast and friction stir processed AZ91 alloy and AZ91/TiC–TiB_2 composite [98]. Reprinted from *Mater. Sci. Eng. A*, Vol. 724, B.N. Sahoo, F. Khan, S. Babu, S.K. Panigrahi, and G.D.J. Ram, Microstructural modification and its effect on strengthening mechanism and yield asymmetry of *in-situ* TiC–TiB_2/AZ91 magnesium matrix composite, 269-282, Copyright 2018, with permission from Elsevier.

As can be seen in the transmission electron microscopy (TEM) images of Fig. 17 [98], material deformation during FSP has led to increased refinement and more homogeneous distribution of the *in-situ* TiC–TiB_2 reinforcing particles, which is a favorable outcome. The tensile stress–strain curves are shown in Fig. 17 [98]. The as-cast AZ91 and AZ91/TiC–TiB_2 exhibited low strength and ductility due to the presence of casting defects and the effects of size, quantity, shape, and distribution of network-type intergranular β-$Mg_{17}Al_{12}$ phase (Fig. 16). However, major improvements in mechanical properties were realized with FSP due to the fragmentation of the coarse β-$Mg_{17}Al_{12}$ phase, grain refinement, and elimination of the inhomogeneous microstructure.

Arora *et al.* [100] fabricated AZ91/TiC–Al_2O_3 hybrid composite by FSP using ball-milled particles that were added by the hole-filling method. Different cooling conditions

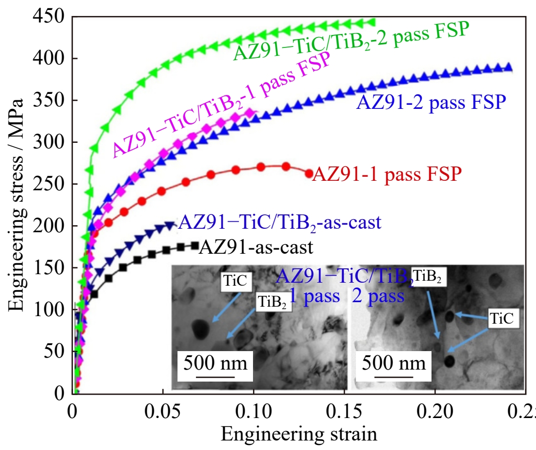

Fig. 17. Tensile stress–strain curves of as-cast and friction stir processed AZ91 alloy and AZ91/TiC–TiB_2 composite as well as some representative TEM images [98]. Reprinted from *Mater. Sci. Eng. A*, Vol. 724, B.N. Sahoo, F. Khan, S. Babu, S.K. Panigrahi, and G.D.J. Ram, Microstructural modification and its effect on strengthening mechanism and yield asymmetry of *in-situ* TiC–TiB_2/AZ91 magnesium matrix composite, 269-282, Copyright 2018, with permission from Elsevier.

were applied for enhanced performance of the material. The results are summarized in Fig. 18, which shows that the hybrid composites have finer grain size and higher hardness compared to the AZ91 alloy. Moreover, the rapid cooling conditions (undersurface cooling using coolant at −20°C) had a greater enhancement effect on both grain refinement and hardness compared to the conventional ambient cooling conditions. FSP processing of AZ91/TiC–Al_2O_3 hybrid composite also led to enhanced scratch resistance [100].

2.6. AZ91–carbon fiber composites

Afrinaldi *et al.* [101] fabricated carbon fiber reinforced AZ91 composite via the addition of chopped carbon fibers with a length of ~1 mm and subsequent FSP (using groove filling and covering method based on a narrow slit). Chopped

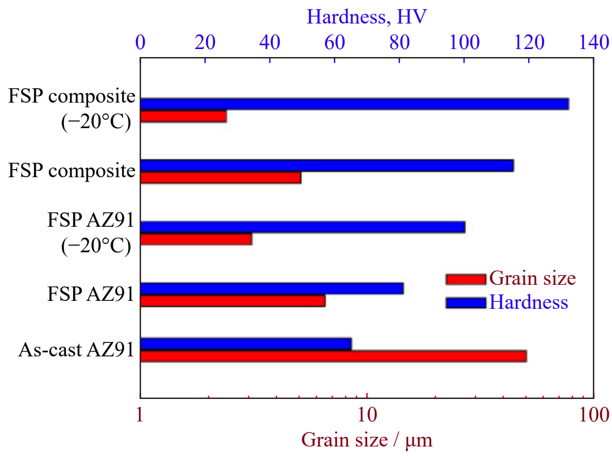

Fig. 18. Grain size and hardness of as-cast and friction stir processed AZ91 alloy and AZ91/TiC–Al_2O_3 composite under different cooling conditions [100]. Adapted by permission from Springer Nature: *Trans. Indian Inst. Met.*, Some investigations on friction stir processed zone of AZ91 alloy, H.S. Arora, H. Singh, B.K. Dhindaw, and H.S. Grewal, Copyright 2012.

carbon fibers were fragmented (to a length of less than 20 μm) and dispersed in the SZ during the FSP process. The effect of the FSP tool was also investigated, where the 3-flat pin tool better reduced the size and number of defects in the SZ compared to the conventional threaded pin tool (Fig. 19(a)). As shown in Fig. 19(b), the fatigue strengths of the carbon fiber-reinforced AZ91 composite were comparable to those of the as-cast counterparts but lower than those of the FSP AZ91 samples without carbon fibers. In fact, fatigue cracks were initiated at the agglomerations of carbon fibers, where the adverse effect of the inhomogeneous distribution of the carbon fibers was also noted.

Mertens *et al.* [102] applied FSP on a sandwich obtained by stacking one layer of C fabric between two sheets of AZ91 alloy. This technique is known as the sandwich method, in which the secondary phase is placed as a laminate or layer between workpieces for subsequent FSP processing [28]. High ω (1500 r/min) and high v (300 mm/min) led to the heterogeneous distribution of the reinforcing phase and high porosity. These defects were more severe for high ω (1500 r/min) and low v (80 mm/min). However, low ω (500 r/min) and low v (80 mm/min) led to the development of a sound processed region with a homogeneous distribution of carbon fibers [102]. These processing conditions were also applied on a sandwich obtained by stacking one layer of C fabric between two sheets of AZ31 alloy. In this case, High ω (1500 r/min) combined with high v (300 mm/min) or low v (80 mm/min) resulted in a sound processed region with a homogeneous distribution of carbon fibers. However, low ω (500 r/min) and low v (80 mm/min) led to the heterogeneous distribution of the reinforcing phase, while low ω (500 r/min) and high v (300 mm/min) resulted in significant porosity. Therefore, while both AZ31 and AZ91 alloys are similar materials, the presence of a high amount of β-$Mg_{17}Al_{12}$ (as well as its dissolution/fragmentation) seems to be an important determinant for the differences as well as for the much smaller processing window for AZ91 composite compared to the AZ31 composite. The AZ91 composite was also found to be capable of age hardening due to the precipitation of the β-$Mg_{17}Al_{12}$ phase (Fig. 20), thus allowing for mechanical behavior improvement after processing [102].

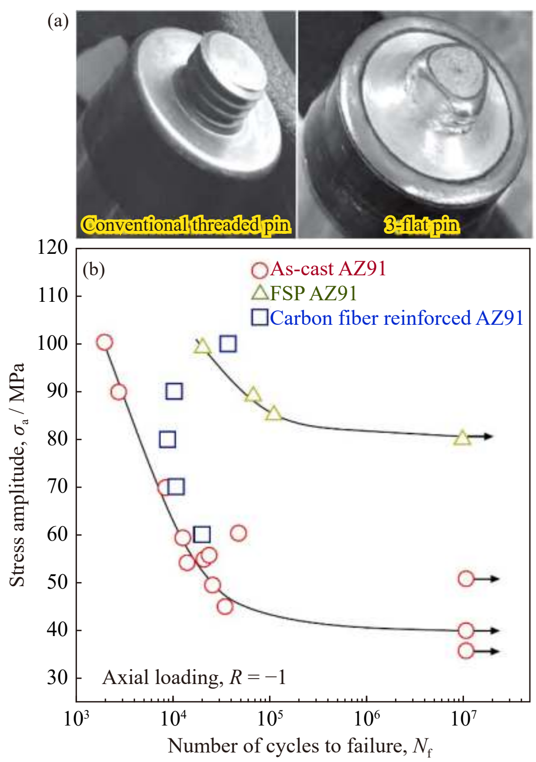

Fig. 19. (a) FSP tools and (b) fatigue *S–N* diagrams of as-cast and friction stir processed AZ91 alloy and AZ91/carbon fiber composite (*R* represents load ratio) [101].

2.7. AZ91–hydroxyapatite composites

Yousefpour *et al.* [103] processed AZ91/hydroxyapatite (HA) bionanocomposites by multipass FSP using the hole filling and covering method. The 2nd and 3rd passes were performed with a 100% overlapping strategy. As shown in Fig. 21, the samples' hardness and strength increased with an increasing number of passes due to better grain refinement and more uniform dispersion of HA powder. Moreover, the introduction of HA powder to AZ91 alloy was found to result in better grain refinement and better mechanical properties. The results of this study clearly show that the particle distribution in the AZ91/HA nanocomposites is significantly affected by the number of FSP passes [103]. In a related study, Yousefpour *et al.* [104] added the hybrid HA/Ag powder, which led to improved grain refining efficiency. Moreover, this sample had the highest texture parameter for the $\{10\bar{1}1\}$ orientation as the high corrosion resistance texture, which was due to the promotion of the nonbasal slip caused by the dissolution of Ag particles in the matrix.

2.8. Other reinforcing phases

Fly ash can be used as an effective reinforcement for fabricating low-cost and environmental-friendly MMCs, as shown by Dinaharan *et al.* [105–106]. In this regard, Patle *et al.* [107] processed AZ91/fly ash surface composite by adding fly ash particles and FSP. Better mechanical and wear properties were realized, but the composite had decreased corrosion resistance for the processed surface composite. Farghadani *et al.* [108] introduced Cu and CuO micropowders on the surface of AZ91 alloy for processing by FSP.

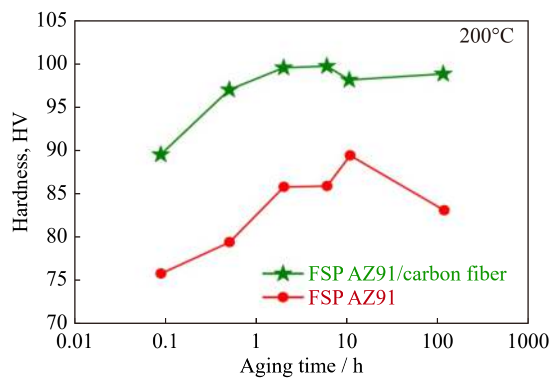

Fig. 20. Hardness at mid-thickness as a function of aging time for friction stir processed AZ91 alloy and AZ91/cabon fiber composite [102].

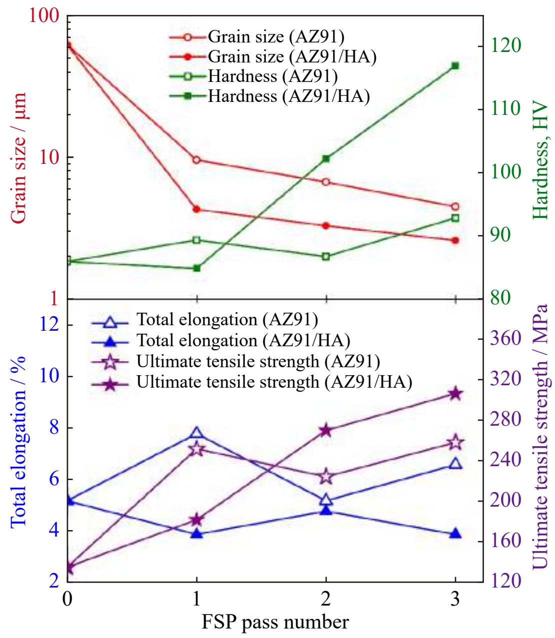

Fig. 21. Grain size and mechanical properties of friction stir processed AZ91 alloy and AZ91/HA composite [103]. Adapted from *J. Mech. Behav. Biomed. Mater.*, Vol. 125, F. Yousefpour, R. Jamaati, and H.J. Aval, Investigation of microstructure, crystallographic texture, and mechanical behavior of magnesium-based nanocomposite fabricated via multi-pass FSP for biomedical applications, 104894, Copyright 2022, with permission from Elsevier.

The AZ91/Cu nanocomposite was reinforced by the *in-situ* formation of the Mg_2Cu compound, while the CuO particles in AZ91/CuO nanocomposite were reduced, and MgO and $MgCu_2$ reinforcing particles were formed alongside the Mg_2Cu compound. Accordingly, grain refinement and *in-situ* formation of reinforcing particles significantly improved the mechanical properties and wear resistance of the composite. Bhadouria *et al.* [109] processed AZ91 hybrid composites via the addition of nano-WC–Co–Cr and multiwalled carbon nanotubes (CNTs) by multipass FSP using the grooving method. The hybrid composites showed better grain refinement, higher hardness, and greater wear resistance compared to the AZ91 alloy and the AZ91/WC–Co–Cr and AZ91/CNTs composites.

3. Future scope/prospects

In the previous section, the reported works on FSP-processed AZ91 composites with SiC, Al_2O_3, SiO_2, B_4C, TiC/TiB_2, carbon fiber, hydroxyapatite, and other reinforcements are summarized. Most of the works are focused on SiC. However, there are many common and effective particles that need to be investigated for AZ91 composites processed by FSP. One of the most common particles is ZrO_2, which has systematically been investigated for FSP AZ31 composites by Chang *et al.* [110], Navazani and Deghani [111], Mazaheri *et al.* [112], Zang *et al.* [113], and Qiao *et al.* [114]. These studies showed that ZrO_2 is a promising particulate for FSP Mg alloys, and hence, systematic investigation of the AZ91/ZrO_2 surface composites by FSP is recommended for future studies. Other important reinforcing phases are CNTs, as demonstrated in the reports of Morisada *et al.* [115], Jamshidijam *et al.* [116], Nia and Nourbakhsh [117], and Arab *et al.* [118] for AZ31 alloy. Based on the results of Bhadouria *et al.* [109], the introduction of CNTs to AZ91 should be further investigated in future works, where issues associated with CNTs, such as agglomeration, need special attention. Recently, Dinaharan *et al.* [86] introduced the titanium particulate-reinforced AZ31 composites for pure Ti [84] and Ti–6Al–4V alloy. Both Ti and Mg have an hcp crystal structure that ensures good compatibility. Moreover, the Ti particulate is deformable and is characterized by a higher elastic modulus, melting point, hardness, and corrosion resistance. Furthermore, the solubility of Ti in magnesium is negligible. As a result, Ti-based particulates seem to be good choices for the processing of Mg-matrix composites. Accordingly, their introduction to AZ91 is an interesting practice for future work. Many other potential reinforcing phases can be added to this list, including graphene nanoplatelets (GNPs) [119–120], ZrB_2 [121], and graphite [122]. Due to their favorable properties, such as wear resistance [123], hybrid composites (with more than one reinforcing phase) have gained considerable attention in recent years [124–125]. The hybrid surface MMCs with more than one reinforcing phase gained attention in material processing due to their noble tribological behavior and surface properties, which cannot be attained in mono composites [99,123]. Several investigators have introduced hybrid reinforcements to the matrix of Mg alloys via FSP, such as Sharma *et al.* [126] (MWCNT–graphene), Jalilvand and Mazaheri [127] (ZrO_2/WC/B_4C), Lu *et al.* [128] (Al_2O_3–CNT), Sahoo *et al.* [98] (TiC–TiB_2), Arora *et al.* [100] (TiC–Al_2O_3), Yousefpour *et al.* [104] (HA–Ag), and Bhadouria *et al.* [109] (WC–Co–Cr–CNTs). Due to the favorable effects of hybrid reinforcements on enhancing the properties of AZ91 alloy, more research in this field is suggested.

As discussed in the previous section, the effects of reinforcement type and particle size, FSP tool geometry, rotation rate, traverse speed, and the number of FSP passes have been investigated for FSP AZ91 composites. However, there are many other variables involved in composite fabrication by FSP [129], as summarized in Table 1. In this regard, the special tool pin profiles have been shown to be favorable [89,130], which need to be investigated for various AZ91 composites. Moreover, much more attention is needed to the effects of particle volume fraction for AZ91 Mg composites [87,109].

For the introduction of reinforcement particles to AZ91 composites, groove filling, hole filling, sandwich method, stir casting, and formation of *in-situ* particles have been applied so far. In fact, the introduction of *in-situ* formed particles in Mg alloys has been observed in several famous systems. The Mg–Si system is the most recognizable one. In this system, Mg_2Si forms during processing [131–132]. Applying FSP on

Table 1. Summary of the variables involved in composite fabrication by FSP

Process parameters	Tool variables	Reinforcement/matrix characteristics
Tool rotation rate	Shoulder diameter	Reinforcement type
Tool traverse speed	Shoulder profile	Reinforcement size
Axial force	Pin profile	Reinforcement volume fraction
Tool tilt angle	Pin diameter	Reinforcement strategy
Plunge depth	Pin length	Mechanical properties of matrix
Number of passes	Tool material	Thermal properties of matrix

the Mg_2Si system is quite effective for enhancing microstructure and mechanical properties through microstructural refinement and modification of primary/eutectic Mg_2Si, as shown by Taghiabadi and Moharami [133] and Raeissi and Nourbaksh [134]. Therefore, it might be interesting to apply FSP to the Si-containing AZ91 alloys [135]. Moreover, the *in-situ* formation of phases is prevalent in many Mg alloys [136], and hence, these alloys might be viewed as composites. For instance, applying FSP to the Mg–Al–Ca system [137] leads to the formation of a fine-grained composite with well-dispersed intermetallic particles (such as the Al_2Ca compound), as shown in Fig. 22 [29]. Therefore, applying FSP to the *in-situ* formed composites is expected to receive considerable attention in the future.

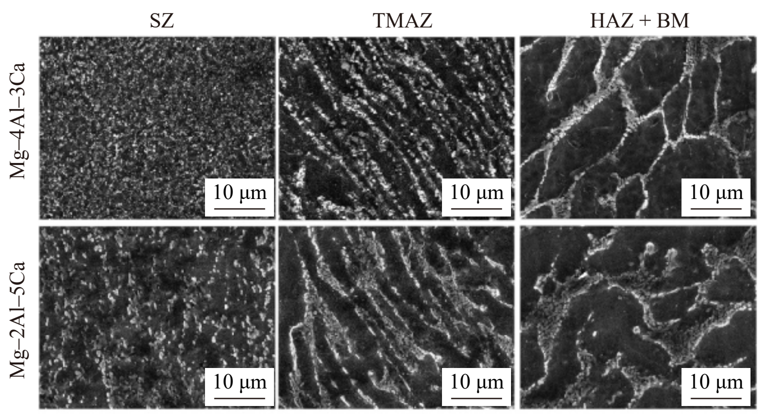

Fig. 22. SEM images of Mg–Al–Ca alloys processed by FSP [29]. Reprinted from *Mater. Lett.*, Vol. 296, Z. Nasiri, M.S. Khorrami, H. Mirzadeh, and M. Emamy, Enhanced mechanical properties of as-cast Mg–Al–Ca magnesium alloys by friction stir processing, 129880, Copyright 2021, with permission from Elsevier.

The dynamically recrystallized grain size is not correlated to the Zener–Hollomon parameter for FSP AZ91 composites (based on Eq. (1)). There is a need for greater attention in future works to determine the effects of particle type and characteristics on grain refinement. The effect of grain size on mechanical strength can be represented by the classical Hall–Petch relationship [138]. This area also needs more research on AZ91 composites to enable a comparison of the results with the obtained values of the Hall–Petch slope for Mg alloys, as summarized by Yu *et al.* [139].

Superplasticity is the ability of a fine-grained polycrystalline material to exhibit very high elongations (≥400%) prior to failure. Since the grain boundary sliding (GBS) is the governing deformation mechanism, the strain rate sensitivity index ($m = \frac{\partial \lg\sigma}{\partial \lg\dot{\varepsilon}}$ based on $\sigma \propto \dot{\varepsilon}^m$) during superplastic flow is ~0.5 [59,140–141]. These large elongations are usually achieved at high temperatures and relatively low strain rates; hence, the grains might become coarse, and superplasticity might be lost due to the replacement of GBS with a dislocation creep mechanism [59]. Accordingly, microduplex or pseudosingle phase alloys are usually considered superplastic materials [142–145]. Friction stir-processed AZ91 magnesium alloy shows better superplastic properties compared to AZ31 alloy due to the higher content of the β-$Mg_{17}Al_{12}$ phase [146]. In fact, FSP can refine the microstructure in the processed region, which is characterized by a high proportion of high-angle grain boundaries as well as particle fragmentation and dispersion. All of these attributes accentuate superplasticity. However, the β-$Mg_{17}Al_{12}$ phase is unstable at elevated temperatures, and its dissolution becomes a drawback to grain growth restriction. As shown in Fig. 23 [147], increasing the deformation temperature from 300 to 350°C accentuates the superplastic properties due to the favorable effect of deformation temperature in obtaining superplasticity at high strain rates (superplasticity at strain rates ≥ 0.01 s^{-1}) [2,59,148]. However, a further increase to 375°C leads to a sharp drop in ductility due to the rapid grain growth. Accordingly, the fine-grained AZ91 nanocomposites processed by FSP with thermally stable reinforcing particles (for grain growth inhibition) might be useful materials for superplastic forming, and this subject needs to be investigated.

Additive manufacturing (AM), which is suitable for the fabrication of a wide range of complex geometries at fine resolutions, is based on the progressive addition of thin layers of materials from 3D model data [149–150]. Besides the most widely used processes in the categories of powder bed fusion and directed energy deposition [151–152], metal AM processes based on friction stir engineering have received considerable attention [153]. These approaches are useful, especially in obtaining Mg alloys that are defect-free with fine-grain size and good mechanical/functional properties [149]. Friction stir AM (FSAM) and additive friction stir deposition are two widely used methods for Mg alloys [150]. These processes seem to be suitable for the processing of composites, which have been examined by Ho *et al.* [154]. Fig. 24 shows the processing of AZ31/hydroxyapatite composites based on FSAM. Accordingly, the applicability of these promising methods for the processing of AZ91 composites is yet to be investigated.

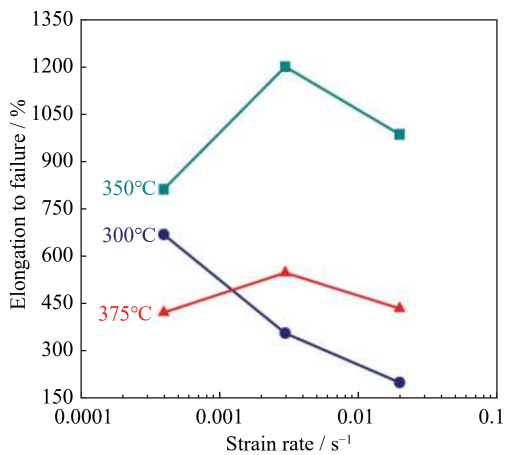

Fig. 23. Tensile elongation vs. strain rate at different temperatures for the submerged friction stir processed AZ91 alloy [147]. Reprinted from *Mater. Sci. Eng. A*, Vol. 568, F. Chai, D.T. Zhang, Y.Y. Li, and W.W. Zhang, High strain rate superplasticity of a fine-grained AZ91 magnesium alloy prepared by submerged friction stir processing, 40-48, Copyright 2013, with permission from Elsevier.

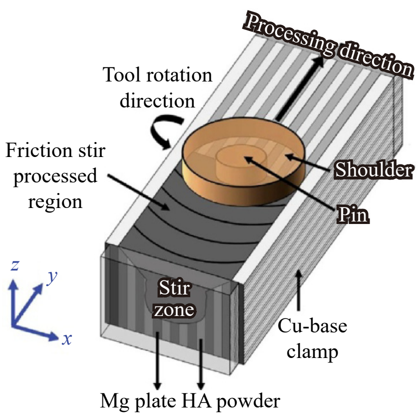

Fig. 24. Processing of AZ31/hydroxyapatite composites by FSAM [154].

4. Summary

In summary, this study reviewed FSP of surface MMCs using the AZ91 alloy, whereby AZ91 composites with various reinforcing phases such as SiC, Al_2O_3, SiO_2, B_4C, TiC, carbon fiber, hydroxyapatite, *in-situ* formed phases, and hybrid reinforcements were critically discussed. FSP composite fabrication methods were discussed, including grooving, hole filling, sandwich method, stir casting followed by FSP, and formation of *in-situ* particles. The effects of introducing second-phase particles and FSP process parameters such as tool rotation rate, traverse speed, number of passes on the microstructural modification, grain refinement, mechanical properties, wear/tribological behavior, and corrosion resistance were also discussed. Finally, useful suggestions were given to shed light on the important issues and to highlight research prospects for future works.

Conflict of Interest

The author declares no conflict of interest.

References

[1] D. Bairagi and S. Mandal, A comprehensive review on biocompatible Mg-based alloys as temporary orthopaedic implants: Current status, challenges, and future prospects, *J. Magnes. Alloys*, 10(2022), No. 3, p. 627.

[2] A. Malik, U.M. Chaudry, K. Hamad, and T.S. Jun, Microstructure features and superplasticity of extruded, rolled and SPD-processed magnesium alloys: A short review, *Metals*, 11(2021), No. 11, art. No. 1766.

[3] B. Pourbahari, H. Mirzadeh, and M. Emamy, Elucidating the effect of intermetallic compounds on the behavior of Mg–Gd–Al–Zn magnesium alloys at elevated temperatures, *J. Mater. Res.*, 32(2017), No. 22, p. 4186.

[4] N. Barri, A.R. Salasel, A. Abbasi, H. Mirzadeh, M. Emamy, and M. Malekan, A new intermetallic phase formation in Mg–Si–Ni magnesium-based *in situ* formed alloys, *Vacuum*, 164(2019), p. 349.

[5] Y. Yang, X.M. Xiong, J. Chen, X.D. Peng, D.L. Chen, and F.S. Pan, Research advances in magnesium and magnesium alloys worldwide in 2020, *J. Magnes. Alloys*, 9(2021), No. 3, p. 705.

[6] Z. Savaedi, H. Mirzadeh, R.M. Aghdam, and R. Mahmudi, Effect of grain size on the mechanical properties and bio-corrosion resistance of pure magnesium, *J. Mater. Res. Technol.*, 19(2022), p. 3100.

[7] E. Gerashi, R. Alizadeh, and R. Mahmudi, Improved corrosion resistance and mechanical properties of biodegradable Mg–4Zn–*x*Sr alloys: Effects of heat treatment, Sr additions, and multi-directional forging, *J. Mater. Res. Technol.*, 20(2022), p. 3363.

[8] Z. Zareian, M. Emamy, M. Malekan, H. Mirzadeh, W.J. Kim, and A. Bahmani, Tailoring the mechanical properties of Mg–Zn magnesium alloy by calcium addition and hot extrusion process, *Mater. Sci. Eng. A*, 774(2020), art. No. 138929.

[9] M. Golrang, M. Mobasheri, H. Mirzadeh, and M. Emamy, Effect of Zn addition on the microstructure and mechanical properties of Mg–0.5Ca–0.5RE magnesium alloy, *J. Alloys Compd.*, 815(2020), art. No. 152380.

[10] J.W. Cha, S.C. Jin, J.G. Jung, and S.H. Park, Effects of homogenization temperature on microstructure and mechanical properties of high-speed-extruded Mg–5Bi–3Al alloy, *J. Magnes. Alloys*, 10(2022), No. 10, p. 2833.

[11] H. Abedi, M. Emamy, J. Rassizadehghani, H. Mirzadeh, and M. Ra'ayatpour, Enhanced mechanical properties of as-cast rare earth bearing magnesium alloy via elevated-temperature

homogenization, *Mater. Today Commun.*, 31(2022), art. No. 103821.

[12] Ö. Ayer, Effect of Die parameters on the grain size, mechanical properties and fracture mechanism of extruded AZ31 magnesium alloys, *Mater. Sci. Eng. A*, 793(2020), art. No. 139887.

[13] M. Razzaghi, H. Mirzadeh, and M. Emamy, Unraveling the effects of Zn addition and hot extrusion process on the microstructure and mechanical properties of as-cast Mg–2Al magnesium alloy, *Vacuum*, 167(2019), p. 214.

[14] J. Dutkiewicz, D. Kalita, W. Maziarz, and M. Faryna, Superplastic deformation of Mg–9Li–2Al–0.5Sc alloy after grain refinement by KoBo extrusion and cyclic forging, *Arch. Civ. Mech. Eng.*, 20(2020), No. 4, p. 1.

[15] I.A. Ibrahim, F.A. Mohamed, and E.J. Lavernia, Particulate reinforced metal matrix composites—A review, *J. Mater. Sci.*, 26(1991), No. 5, p. 1137.

[16] M. Maleki, H. Mirzadeh, and M. Emamy, Improvement of mechanical properties of *in situ* Mg–Si composites via Cu addition and hot working, *J. Alloys Compd.*, 905(2022), art. No. 164176.

[17] C.J. AnandhaKumar, S. Gopi, D.G. Mohan, and S. ShashiKumar, Predicting the ultimate tensile strength and wear rate of aluminium hybrid surface composites fabricated via friction stir processing using computational methods, *J. Adhesion Sci. Technol.*, 36(2022), No. 16, p. 1707.

[18] S.J. Chen, L. Wang, X.Q. Jiang, T. Yuan, W. Jiang, and Y.Y. Liu, Microstructure and mechanical properties of AZ31B Mg alloy fabricated by friction stir welding with pulse current, *J. Manuf. Processes*, 71(2021), p. 317.

[19] R.S. Mishra and Z.Y. Ma, Friction stir welding and processing, *Mater. Sci. Eng. R*, 50(2005), No. 1-2, p. 1.

[20] A. Heidarzadeh, S. Mironov, R. Kaibyshev, *et al.*, Friction stir welding/processing of metals and alloys: A comprehensive review on microstructural evolution, *Prog. Mater. Sci.*, 117(2021), art. No. 100752.

[21] V. Patel, W.Y. Li, A. Vairis, and V. Badheka, Recent development in friction stir processing as a solid-state grain refinement technique: Microstructural evolution and property enhancement, *Crit. Rev. Solid State Mater. Sci.*, 44(2019), No. 5, p. 378.

[22] B. Sadeghi, M. Shamanian, F. Ashrafizadeh, P. Cavaliere, and A. Rizzo, Friction stir processing of spark plasma sintered aluminum matrix composites with bimodal micro- and nano-sized reinforcing Al_2O_3 particles, *J. Manuf. Processes*, 32(2018), p. 412.

[23] G. Moeini, S.V. Sajadifar, T. Wegener, *et al.*, On the influence of build orientation on properties of friction stir welded Al–Si10Mg parts produced by selective laser melting, *J. Mater. Res. Technol.*, 12(2021), p. 1446.

[24] D. Harwani, V. Badheka, V. Patel, W.Y. Li, and J. Andersson, Developing superplasticity in magnesium alloys with the help of friction stir processing and its variants - A review, *J. Mater. Res. Technol.*, 12(2021), p. 2055.

[25] A.K. Srivastava, A.R. Dixit, M. Maurya, *et al.*, 20th century uninterrupted growth in friction stir processing of lightweight composites and alloys, *Mater. Chem. Phys.*, 266(2021), art. No. 124572.

[26] R.S. Mishra, Z.Y. Ma, and I. Charit, Friction stir processing: A novel technique for fabrication of surface composite, *Mater. Sci. Eng. A*, 341(2003), No. 1-2, p. 307.

[27] S. Bharti, N.D. Ghetiya, and K.M. Patel, A review on manufacturing the surface composites by friction stir processing, *Mater. Manuf. Processes*, 36(2021), No. 2, p. 135.

[28] B.R. Sunil, G.P.K. Reddy, H. Patle, and R. Dumpala, Magnesium based surface metal matrix composites by friction stir processing, *J. Magnes. Alloys*, 4(2016), No. 1, p. 52.

[29] Z. Nasiri, M.S. Khorrami, H. Mirzadeh, and M. Emamy, Enhanced mechanical properties of as-cast Mg–Al–Ca magnesium alloys by friction stir processing, *Mater. Lett.*, 296(2021), art. No. 129880.

[30] M.N. Avettand-Fènoël and A. Simar, A review about friction stir welding of metal matrix composites, *Mater. Charact.*, 120(2016), p. 1.

[31] W. Tang, X. Guo, J.C. McClure, L.E. Murr, and A. Nunes, Heat input and temperature distribution in friction stir welding, *J. Mater. Process. Manuf. Sci.*, 7(1998), No. 2, p. 163.

[32] R. Rouzbehani, A.H. Kokabi, H. Sabet, M. Paidar, and O.O. Ojo, Metallurgical and mechanical properties of underwater friction stir welds of Al7075 aluminum alloy, *J. Mater. Process. Technol.*, 262(2018), p. 239.

[33] F. Badkoobeh, H. Mostaan, M. Rafiei, H.R. Bakhsheshi-Rad, and F. Berto, Friction stir welding/processing of Mg-based alloys: A critical review on advancements and challenges, *Materials*, 14(2021), No. 21, art. No. 6726.

[34] Y.X. Huang, T.H. Wang, W.Q. Guo, L. Wan and S.X. Lv, Microstructure and surface mechanical property of AZ31 Mg/SiC_p surface composite fabricated by direct friction stir processing, *Mater. Des.*, 59(2014), p. 274.

[35] A.I. Almazrouee, K.J. Al-Fadhalah, and S.N. Alhajeri, A new approach to direct friction stir processing for fabricating surface composites, *Crystals*, 11(2021), No. 6, art. No. 638.

[36] J. Iwaszko and M. Sajed, Technological aspects of producing surface composites by friction stir processing—A review, *J. Compos. Sci.*, 5(2021), No. 12, art. No. 323.

[37] D. Sejani, W.Y. Li, and V. Patel, Stationary shoulder friction stir welding–low heat input joining technique: A review in comparison with conventional FSW and bobbin tool FSW, *Crit. Rev. Solid State Mater. Sci.*, 47(2022), No. 6, p. 865.

[38] V. Patel, W.Y. Li, and Y.X. Xu, Stationary shoulder tool in friction stir processing: A novel low heat input tooling system for magnesium alloy, *Mater. Manuf. Processes*, 34(2019), No. 2, p. 177.

[39] V. Patel, W.Y. Li, J. Andersson, and N. Li, Enhancing grain refinement and corrosion behavior in AZ31B magnesium alloy via stationary shoulder friction stir processing, *J. Mater. Res. Technol.*, 17(2022), p. 3150.

[40] V. Patel, W.Y. Li, and Q. Wen, Surface analysis of stationary shoulder friction stir processed AZ31B magnesium alloy, *Mater. Sci. Technol.*, 35(2019), No. 5, p. 628.

[41] W.Y. Li, P.L. Niu, S.R. Yan, V. Patel, and Q. Wen, Improving microstructural and tensile properties of AZ31B magnesium alloy joints by stationary shoulder friction stir welding, *J. Manuf. Processes*, 37(2019), p. 159.

[42] F. Yousefpour, R. Jamaati, and H.J. Aval, Effect of traverse and rotational speeds on microstructure, texture, and mechanical properties of friction stir processed AZ91 alloy, *Mater. Charact.*, 178(2021), art. No. 111235.

[43] H.J. Sharahi, M. Pouranvari, and M. Movahedi, Strengthening and ductilization mechanisms of friction stir processed cast Mg–Al–Zn alloy, *Mater. Sci. Eng. A*, 781(2020), art. No. 139249.

[44] A. Afsharnaderi, M. Lotfpour, H. Mirzadeh, M. Emamy, and M. Malekan, Enhanced mechanical properties of as-cast AZ91 magnesium alloy by combined RE–Sr addition and hot extrusion, *Mater. Sci. Eng. A*, 792(2020), art. No. 139817.

[45] F. Ghorbani, M. Emamy, and H. Mirzadeh, Enhanced tensile properties of as-cast Mg–10Al magnesium alloy via strontium addition and hot working, *Arch. Civ. Mech. Eng.*, 21(2021), No. 2, p. 1.

[46] H. Mirzadeh, A comparative study on the hot flow stress of Mg–Al–Zn magnesium alloys using a simple physically-based approach, *J. Magnes. Alloys*, 2(2014), No. 3, p. 225.

[47] S. Rathee, S. Maheshwari, A.N. Siddiquee, and M. Srivastava, A review of recent progress in solid state fabrication of com-

posites and functionally graded systems via friction stir processing, *Crit. Rev. Solid State Mater. Sci.*, 43(2018), No. 4, p. 334.
[48] Q. Liu, Q.X. Ma, G.Q. Chen, *et al*., Enhanced corrosion resistance of AZ91 magnesium alloy through refinement and homogenization of surface microstructure by friction stir processing, *Corros. Sci.*, 138(2018), p. 284.
[49] F. Chai, F. Yan, W. Wang, Q.C. Lu, and X. Fang, Microstructures and mechanical properties of AZ91 alloys prepared by multi-pass friction stir processing, *J. Mater. Res.*, 33(2018), No. 12, p. 1789.
[50] P. Asadi, M.K.B. Givi, K. Abrinia, M. Taherishargh, and R. Salekrostam, Effects of SiC particle size and process parameters on the microstructure and hardness of AZ91/SiC composite layer fabricated by FSP, *J. Mater. Eng. Perform.*, 20(2011), No. 9, p. 1554.
[51] J. Iwaszko, K. Kudła, and K. Fila, Friction stir processing of the AZ91 magnesium alloy with SiC particles, *Arch. Mater. Sci. Eng.*, 77(2016), No. 2, p. 85.
[52] P. Asadi, G. Faraji, A. Masoumi, and M.K.B. Givi, Experimental investigation of magnesium-base nanocomposite produced by friction stir processing: Effects of particle types and number of friction stir processing passes, *Metall. Mater. Trans. A*, 42(2011), No. 9, p. 2820.
[53] M. Dadaei, H. Omidvar, B. Bagheri, M. Jahazi, and M. Abbasi, The effect of SiC/Al_2O_3 particles used during FSP on mechanical properties of AZ91 magnesium alloy, *Int. J. Mater. Res.*, 105(2014), No. 4, p. 369.
[54] B. Bagheri, M. Abbasi, A. Abdollahzadeh, and S.E. Mirsalehi, Effect of second-phase particle size and presence of vibration on AZ91/SiC surface composite layer produced by FSP, *Trans. Nonferrous Met. Soc. China*, 30(2020), No. 4, p. 905.
[55] Z. Savaedi, R. Motallebi, and H. Mirzadeh, A review of hot deformation behavior and constitutive models to predict flow stress of high-entropy alloys, *J. Alloys Compd.*, 903(2022), art. No. 163964.
[56] A.H. Ammouri, G. Kridli, G. Ayoub, and R.F. Hamade, Relating grain size to the Zener–Hollomon parameter for twin-roll-cast AZ31B alloy refined by friction stir processing, *J. Mater. Process. Technol.*, 222(2015), p. 301.
[57] H. Mirzadeh, Developing constitutive equations of flow stress for hot deformation of AZ31 magnesium alloy under compression, torsion, and tension, *Int. J. Mater. Form.*, 12(2019), No. 4, p. 643.
[58] L. Commin, M. Dumont, J.E. Masse, and L. Barrallier, Friction stir welding of AZ31 magnesium alloy rolled sheets: Influence of processing parameters, *Acta Mater.*, 57(2009), No. 2, p. 326.
[59] H. Mirzadeh, High strain rate superplasticity via friction stir processing (FSP): A review, *Mater. Sci. Eng. A*, 819(2021), art. No. 141499.
[60] C.I. Chang, C.J. Lee, and J.C. Huang, Relationship between grain size and Zener–Holloman parameter during friction stir processing in AZ31 Mg alloys, *Scripta Mater.*, 51(2004), No. 6, p. 509.
[61] K. Dehghani and A. Chabok, Dependence of Zener parameter on the nanograins formed during friction stir processing of interstitial free steels, *Mater. Sci. Eng. A*, 528(2011), No. 13-14, p. 4325.
[62] A.M. Jamili, A. Zarei-Hanzaki, H.R. Abedi, M. Mosayebi, R. Kocich, and L.Kunčická, Development of fresh and fully recrystallized microstructures through friction stir processing of a rare earth bearing magnesium alloy, *Mater. Sci. Eng. A*, 775(2020), art. No. 138837.
[63] B. Bagheri, M. Abbasi, A. Abdollahzadeh, and A.H. Kokabi, A comparative study between friction stir processing and friction stir vibration processing to develop magnesium surface nanocomposites, *Int. J. Miner. Metall. Mater.*, 27(2020), No. 8, p. 1133.
[64] J. Iwaszko and K. Kudła, Microstructure, hardness, and wear resistance of AZ91 magnesium alloy produced by friction stir processing with air-cooling, *Int. J. Adv. Manuf. Technol.*, 116(2021), No. 3-4, p. 1309.
[65] J. Iwaszko, New trends in friction stir processing: Rapid cooling—A review, *Trans. Indian Inst. Met.*, 75(2022), No. 7, p. 1681.
[66] C. Rathinasuriyan, A. Mystica, R. Sankar, and V.S.S. Kumar, Experimental investigation of cooling medium on submerged friction stir processed AZ31 magnesium alloy, *Mater. Today Proc.*, 46(2021), p. 3386.
[67] V. Patel, W.Y. Li, X.C. Liu, *et al*., Tailoring grain refinement through thickness in magnesium alloy via stationary shoulder friction stir processing and copper backing plate, *Mater. Sci. Eng. A*, 784(2020), art. No. 139322.
[68] J.L. Shang, L.M. Ke, F.C. Liu, F.Y. Lv, and L. Xing, Aging behavior of nano SiC particles reinforced AZ91D composite fabricated via friction stir processing, *J. Alloys Compd.*, 797(2019), p. 1240.
[69] M. Rabiee, H. Mirzadeh, and A. Ataie, Processing of Cu–Fe and Cu–Fe–SiC nanocomposites by mechanical alloying, *Adv. Powder Technol.*, 28(2017), No. 8, p. 1882.
[70] T.J. Chen, Z.M. Zhu, Y. Ma, Y.D. Li, and Y. Hao, Friction stir processing of thixoformed AZ91D magnesium alloy and fabrication of surface composite reinforced by SiC_ps, *J. Wuhan Univ. Technol. Mater. Sci. Ed.*, 25(2010), No. 2, p. 223.
[71] W.B. Lee, C.Y. Lee, M.K. Kim, *et al*., Microstructures and wear property of friction stir welded AZ91 Mg/SiC particle reinforced composite, *Compos. Sci. Technol.*, 66(2006), No. 11-12, p. 1513.
[72] M. Abbasi, B. Bagheri, M. Dadaei, H.R. Omidvar, and M. Rezaei, The effect of FSP on mechanical, tribological, and corrosion behavior of composite layer developed on magnesium AZ91 alloy surface, *Int. J. Adv. Manuf. Technol.*, 77(2015), No. 9-12, p. 2051.
[73] A. Abdollahzadeh, B. Bagheri, M. Abbasi, F. Sharifi, and A.O. Moghaddam, Mechanical, wear and corrosion behaviors of AZ91/SiC composite layer fabricated by friction stir vibration processing, *Surf. Topogr.: Metrol. Prop.*, 9(2021), No. 3, art. No. 035038.
[74] G. Faraji, O. Dastani, and S.A.A.A. Mousavi, Microstructures and mechanical properties of Al_2O_3/AZ91 surface nanocomposite layer produced by friction stir processing, *Proc. Inst. Mech. Eng. B J. Eng. Manuf.*, 225(2011), No. 8, p. 1331.
[75] G. Faraji, O. Dastani, and S.A.A.A. Mousavi, Effect of process parameters on microstructure and micro-hardness of AZ91/Al_2O_3 surface composite produced by FSP, *J. Mater. Eng. Perform.*, 20(2011), No. 9, p. 1583.
[76] D. Ahmadkhaniha, M.H. Sohi, A. Salehi, and R. Tahavvori, Formations of AZ91/Al_2O_3 nano-composite layer by friction stir processing, *J. Magnes. Alloys*, 4(2016), No. 4, p. 314.
[77] M. Soleimani, H. Mirzadeh, and C. Dehghanian, Processing route effects on the mechanical and corrosion properties of dual phase steel, *Met. Mater. Int.*, 26(2020), No. 6, p. 882.
[78] V.R. Vaira, R. Padmanaban, and M. Govindaraju, Synthesis and characterization of magnesium alloy surface composite (AZ91D–SiO_2) by friction stir processing for bioimplants, *Silicon*, 12(2020), No. 5, p. 1085.
[79] D. Khayyamin, A. Mostafapour, and R. Keshmiri, The effect of process parameters on microstructural characteristics of AZ91/SiO_2 composite fabricated by FSP, *Mater. Sci. Eng. A*, 559(2013), p. 217.
[80] Z. Savaedi, H. Mirzadeh, R.M. Aghdam, and R. Mahmudi, Thermal stability, grain growth kinetics, mechanical properties, and bio-corrosion resistance of pure Mg, ZK30, and

ZEK300 alloys: A comparative study, *Mater. Today Commun.*, 33(2022), art. No. 104825.
[81] M.R. Zamani, H. Mirzadeh, M. Malekan, S.C. Cao, and J.W. Yeh, Grain growth in high-entropy alloys (HEAs): A review, *High Entropy Alloys Mater.*, 2022. https://doi.org/10.1007/s44210-022-00002-8
[82] I. Dinaharan, N. Murugan, and E.T. Akinlabi, Friction stir processing route for metallic matrix composite production, [in] *Encyclopedia of Materials: Composites*, Vol. 2, Elsevier, Amsterdam, 2021, p. 702.
[83] M. Rezayat, M. Gharechomaghlu, H. Mirzadeh, and M.H. Parsa, A comprehensive approach for quantitative characterization and modeling of composite microstructures, *Appl. Math. Model.*, 40(2016), No. 19-20, p. 8826.
[84] I. Dinaharan, S. Zhang, G.Q. Chen, and Q.Y. Shi, Development of titanium particulate reinforced AZ31 magnesium matrix composites via friction stir processing, *J. Alloys Compd.*, 820(2020), art. No. 153071.
[85] V. Sharma, Y. Gupta, B.V.M. Kumar, and U. Prakash, Friction stir processing strategies for uniform distribution of reinforcement in a surface composite, *Mater. Manuf. Processes*, 31(2016), No. 10, p. 1384.
[86] I. Dinaharan, S. Zhang, G.Q. Chen, and Q.Y. Shi, Assessment of Ti–6Al–4V particles as a reinforcement for AZ31 magnesium alloy-based composites to boost ductility incorporated through friction stir processing, *J. Magnes. Alloys*, 10(2022), No. 4, p. 979.
[87] I. Dinaharan, S. Zhang, G.Q. Chen, and Q.Y. Shi, Titanium particulate reinforced AZ31 magnesium matrix composites with improved ductility prepared using friction stir processing, *Mater. Sci. Eng. A*, 772(2020), art. No. 138793.
[88] W. Wang, P. Han, P. Peng, *et al.*, Friction stir processing of magnesium alloys: A review, *Acta Metall. Sin. Engl. Lett.*, 33(2020), No. 1, p. 43.
[89] A.M. Desai, B.C. Khatri, V. Patel, and H. Rana, Friction stir welding of AZ31 magnesium alloy: A review, *Mater. Today Proc.*, 47(2021), p. 6576.
[90] P. Asadi, M.K.B. Givi, N. Parvin, A. Araei, M. Taherishargh, and S. Tutunchilar, On the role of cooling and tool rotational direction on microstructure and mechanical properties of friction stir processed AZ91, *Int. J. Adv. Manuf. Technol.*, 63(2012), No. 9-12, p. 987.
[91] K. Fuse, V. Badheka, V. Patel, and J. Andersson, Dual sided composite formation in Al6061/B_4C using novel bobbin tool friction stir processing, *J. Mater. Res. Technol.*, 13(2021), p. 1709.
[92] S. Rathee, S. Maheshwari, A.N. Siddiquee, and M. Srivastava, Effect of tool plunge depth on reinforcement particles distribution in surface composite fabrication via friction stir processing, *Def. Technol.*, 13(2017), No. 2, p. 86.
[93] M. Balakrishnan, I. Dinaharan, R. Palanivel, and R. Sivaprakasam, Synthesize of AZ31/TiC magnesium matrix composites using friction stir processing, *J. Magnes. Alloys*, 3(2015), No. 1, p. 76.
[94] K. Wei, R. Hu, D.D. Yin, *et al.*, Grain size effect on tensile properties and slip systems of pure magnesium, *Acta Mater.*, 206(2021), art. No. 116604.
[95] H. Patle, B.R. Sunil, and R. Dumpala, Sliding wear behavior of AZ91/B_4C surface composites produced by friction stir processing, *Mater. Res. Express*, 7(2020), No. 1, art. No. 016586.
[96] N. Singh, J. Singh, B. Singh, and N. Singh, Wear behavior of B_4C reinforced AZ91 matrix composite fabricated by FSP, *Mater. Today Proc.*, 5(2018), No. 9, p. 19976.
[97] S. Vijayan, J.P.L. Gnanavel, G. Selvakumar, and S.R.K. Rao, Study on surface characteristics of friction stir processed AZ91 with titanium carbide micro particles, *Indian J. Eng. Mater. Sci.*, 26(2019), No. 3-4, p. 205.
[98] B.N. Sahoo, M.D.F. Khan, S. Babu, S.K. Panigrahi, and G.D.J. Ram, Microstructural modification and its effect on strengthening mechanism and yield asymmetry of *in situ* TiC–TiB_2/AZ91 magnesium matrix composite, *Mater. Sci. Eng. A*, 724(2018), p. 269.
[99] M.R. Moazami, A. Razaghian, H. Mirzadeh, M. Emamy, and A. Moharami, Tribological behavior of as-cast and wrought Al–Mg_2Si hybrid composites reinforced by Ti-based intermetallics, *J. Mater. Res. Technol.*, 20(2022), p. 1315.
[100] H.S. Arora, H. Singh, B.K. Dhindaw, and H.S. Grewal, Some investigations on friction stir processed zone of AZ91 alloy, *Trans. Indian Inst. Met.*, 65(2012), No. 6, p. 735.
[101] A. Afrinaldi, T. Kakiuchi, S. Nakagawa, *et al.*, Fabrication of recycled carbon fiber reinforced magnesium alloy composite by friction stir processing using 3-flat pin tool and its fatigue properties, *Mater. Trans.*, 59(2018), No. 3, p. 475.
[102] A.I. Mertens, A. Simar, H.M. Montrieux, J. Halleux, F. Delannay, and J. Lecomte-Beckers, Friction stir processing of magnesium matrix composites reinforced with carbon fibres: Influence of the matrix characteristics and of the processing parameters on microstructural developments, [in] *9th International Conference on Mgnesium Alloys and their Applications*, Vancouver, 2012.
[103] F. Yousefpour, R. Jamaati, and H.J. Aval, Investigation of microstructure, crystallographic texture, and mechanical behavior of magnesium-based nanocomposite fabricated via multipass FSP for biomedical applications, *J. Mech. Behav. Biomed. Mater.*, 125(2022), art. No. 104894.
[104] F. Yousefpour, R. Jamaati, and H.J. Aval, Synergistic effects of hybrid (HA+Ag) particles and friction stir processing in the design of a high-strength magnesium matrix bio-nano composite with an appropriate texture for biomedical applications, *J. Mech. Behav. Biomed. Mater.*, 125(2022), art. No. 104983.
[105] I. Dinaharan and E.T. Akinlabi, Low cost metal matrix composites based on aluminum, magnesium and copper reinforced with fly ash prepared using friction stir processing, *Compos. Commun.*, 9(2018), p. 22.
[106] I. Dinaharan, S.C. Vettivel, M. Balakrishnan, and E.T. Akinlabi, Influence of processing route on microstructure and wear resistance of fly ash reinforced AZ31 magnesium matrix composites, *J. Magnes. Alloys*, 7(2019), No. 1, p. 155.
[107] H. Patle, B.R. Sunil, and R. Dumpala, Machining characteristics, wear and corrosion behavior of AZ91 magnesium alloy–fly ash composites produced by friction stir processing, *Materialwiss. Werkstofftech.*, 52(2021), No. 1, p. 88.
[108] M. Farghadani, F. Karimzadeh, M.H. Enayati, N. Naghshehkesh, and A.O. Moghaddam, Fabrication of AZ91D/Cu/Mg_2Cu and AZ91D/Mg_2Cu/$MgCu_2$/MgO *in situ* hybrid surface nanocomposites via friction stir processing, *Surf. Topogr.: Metrol. Prop.*, 8(2020), No. 4, art. No. 045002.
[109] N. Bhadouria, P. Kumar, L. Thakur, S. Dixit, and N. Arora, A study on micro-hardness and tribological behaviour of nano-WC–Co–Cr/multi-walled carbon nanotubes reinforced AZ91D magnesium matrix surface composites, *Trans. Indian Inst. Met.*, 70(2017), No. 9, p. 2477.
[110] C.I. Chang, Y.N. Wang, H.R. Pei, C.J. Lee, and J.C. Huang, On the hardening of friction stir processed Mg-AZ31 based composites with 5–20% nano-ZrO_2 and nano-SiO_2 particles, *Mater. Trans.*, 47(2006), No. 12, p. 2942.
[111] M. Navazani and K. Dehghani, Fabrication of Mg–ZrO_2 surface layer composites by friction stir processing, *J. Mater. Process. Technol.*, 229(2016), p. 439.
[112] Y. Mazaheri, M.M. Jalilvand, A. Heidarpour, and A.R. Jahani, Tribological behavior of AZ31/ZrO_2 surface nanocomposites developed by friction stir processing, *Tribol. Int.*, 143(2020), art. No. 106062.
[113] Q.H. Zang, X.W. Li, H.M. Chen, *et al.*, Microstructure and

mechanical properties of AZ31/ZrO_2 composites prepared by friction stir processing with high rotation speed, *Front. Mater.*, 7(2020), art. No. 278.

[114] K. Qiao, T. Zhang, K.S. Wang, *et al*., Effect of multi-pass friction stir processing on the microstructure evolution and corrosion behavior of ZrO_2/AZ31 magnesium matrix composite, *J. Mater. Res. Technol.*, 18(2022), p. 1166.

[115] Y. Morisada, H. Fujii, T. Nagaoka, and M. Fukusumi, MWCNTs/AZ31 surface composites fabricated by friction stir processing, *Mater. Sci. Eng. A*, 419(2006), No. 1-2, p. 344.

[116] M. Jamshidijam, A. Akbari-Fakhrabadi, S.M. Masoudpanah, G.H. Hasani, and R.V. Mangalaraja, Wear behavior of multiwalled carbon nanotube/AZ31 composite obtained by friction stir processing, *Tribol. Trans.*, 56(2013), No. 5, p. 827.

[117] A.A. Nia and S.H. Nourbakhsh, Microstructure and mechanical properties of AZ31/SiC and AZ31/CNT composites produced by friction stir processing, *Trans. Indian Inst. Met.*, 69(2016), No. 7, p. 1435.

[118] S.M. Arab, S.M. Zebarjad, and S.A.J. Jahromi, Fabrication of AZ31/MWCNTs surface metal matrix composites by friction stir processing: Investigation of microstructure and mechanical properties, *J. Mater. Eng. Perform.*, 26(2017), No. 11, p. 5366.

[119] M. Tabandeh-Khorshid, A. Kumar, E. Omrani, C. Kim, and P. Rohatgi, Synthesis, characterization, and properties of graphene reinforced metal-matrix nanocomposites, *Composites Part B*, 183(2020), art. No. 107664.

[120] Y.M. Xie, X.C. Meng Y.X. Huang, J.C. Li, and J. Cao, Deformation-driven metallurgy of graphene nanoplatelets reinforced aluminum composite for the balance between strength and ductility, *Composites Part B*, 177(2019), art. No. 107413.

[121] N. Babu and A. Megalingam, Microstructural, mechanical and tribological characterization of ZrB_2 reinforced AZ31B surface coatings made by friction stir processing, *J. Adhesion Sci. Technol.*, 37(2023), No. 2, p. 195.

[122] K.V. Reddy, R.B. Naik, G.R. Rao, G.M. Reddy, and R.A. Kumar, Microstructure and damping capacity of AA6061/graphite surface composites produced through friction stir processing, *Compos. Commun.*, 20(2020), art. No. 100352.

[123] D.K. Sharma, V. Badheka, V. Patel, and G. Upadhyay, Recent developments in hybrid surface metal matrix composites produced by friction stir processing: A review, *J. Tribol.*, 143(2021), No. 5, art. No. 050801.

[124] M.Y. Zhou, L.B. Ren, L.L. Fan, *et al*., Progress in research on hybrid metal matrix composites, *J. Alloys Compd.*, 838(2020), art. No. 155274.

[125] F. Khorasani, M. Emamy, M. Malekan, *et al*., Enhancement of the microstructure and elevated temperature mechanical properties of as-cast Mg–Al_2Ca–Mg_2Ca *in situ* composite by hot extrusion, *Mater. Charact.*, 147(2019), p. 155.

[126] S. Sharma, A. Handa, S.S. Singh, and D. Verma, Influence of tool rotation speeds on mechanical and morphological properties of friction stir processed nano hybrid composite of MWCNT–graphene–AZ31 magnesium, *J. Magnes. Alloys*, 7(2019), No. 3, p. 487.

[127] M.M. Jalilvand, and Y. Mazaheri, Effect of mono and hybrid ceramic reinforcement particles on the tribological behavior of the AZ31 matrix surface composites developed by friction stir processing, *Ceram. Int.*, 46(2020), No. 12, p. 20345.

[128] D.H. Lu, Y.H. Jiang, and R. Zhou, Wear performance of nano-Al_2O_3 particles and CNTs reinforced magnesium matrix composites by friction stir processing, *Wear*, 305(2013), No. 1-2, p. 286.

[129] S. Rathee, S. Maheshwari, and A.N. Siddiquee, Issues and strategies in composite fabrication via friction stir processing: A review, *Mater. Manuf. Processes*, 33(2018), No. 3, p. 239.

[130] R. Palanivel, P.K. Mathews, N. Murugan, and I. Dinaharan, Effect of tool rotational speed and pin profile on microstructure and tensile strength of dissimilar friction stir welded AA5083-H111 and AA6351-T6 aluminum alloys, *Mater. Des.*, 40(2012), p. 7.

[131] M. Lotfpour, A. Bahmani, H. Mirzadeh, *et al*., Effect of microalloying by Ca on the microstructure and mechanical properties of as-cast and wrought Mg–Mg_2Si composites, *Mater. Sci. Eng. A*, 820(2021), art. No. 141574.

[132] A.R. Salasel, A. Abbasi, N. Barri, H. Mirzadeh, M. Emamy, and M. Malekan, Effect of Si and Ni on microstructure and mechanical properties of *in situ* magnesium-based composites in the as-cast and extruded conditions, *Mater. Chem. Phys.*, 232(2019), p. 305.

[133] R. Taghiabadi and A. Moharami, Mechanical properties enhancement of Mg–4Si *in situ* composites by friction stir processing, *Mater. Sci. Technol.*, 37(2021), No. 1, p. 66.

[134] M. Raeissi and S.H. Nourbaksh, Enhancement of the microstructure homogeneity and mechanical performance of the as-cast Mg/Mg_2Si *in-situ* composite through friction stir processing, *Mater. Res. Express*, 6(2019), No. 10, art. No. 1065e7.

[135] A. Srinivasan, S. Ningshen, U.K. Mudali, U.T.S. Pillai, and B.C. Pai, Influence of Si and Sb additions on the corrosion behavior of AZ91 magnesium alloy, *Intermetallics*, 15(2007), No. 12, p. 1511.

[136] K.B. Nie, X.J. Wang, K.K. Deng, X.S. Hu, and K. Wu, Magnesium matrix composite reinforced by nanoparticles–A review, *J. Magnes. Alloys*, 9(2021), No. 1, p. 57.

[137] Z. Nasiri, H. Mirzadeh, M.S. Khorrami, and M. Emamy, Synergistic effects of alloying, homogenization, and hot extrusion on the mechanical properties of as-cast Mg–Al–Ca magnesium alloys, *Arch. Civ. Mech. Eng.*, 21(2021), No. 3, art. No. 126.

[138] M.S. Mehranpour, A. Heydarinia, M. Emamy, H. Mirzadeh, A. Koushki, and R. Razi, Enhanced mechanical properties of AZ91 magnesium alloy by inoculation and hot deformation, *Mater. Sci. Eng. A*, 802(2021), art. No. 140667.

[139] H.H. Yu, Y.C. Xin, M.Y. Wang, and Q. Liu, Hall-Petch relationship in Mg alloys: A review, *J. Mater. Sci. Technol.*, 34(2018), No. 2, p. 248.

[140] T.G. Langdon, Seventy-five years of superplasticity: Historic developments and new opportunities, *J. Mater. Sci.*, 44(2009), No. 22, p. 5998.

[141] Z. Savaedi, R. Motallebi, H. Mirzadeh, and M. Malekan, Superplasticity of bulk metallic glasses (BMGs): A review, *J. Non Cryst. Solids*, 583(2022), art. No. 121503.

[142] R. Motallebi, Z. Savaedi, and H. Mirzadeh, Superplasticity of high-entropy alloys: A review, *Arch. Civ. Mech. Eng.*, 22(2021), No. 1, p. 1.

[143] G. Giuliano, *Superplastic Forming of Advanced Metallic Materials: Methods and Applications*, Woodhead Publishing Limited, Cambridge, 2011.

[144] M. Sabbaghian and R. Mahmudi, Superplasticity of the fine-grained friction stir processed Mg–3Gd–1Zn sheets, *Mater. Charact.*, 172(2021), art. No. 110902.

[145] M.M. Hoseini-Athar, R. Mahmudi, R.P. Babu, and P. Hedström, Microstructure and superplasticity of Mg–2Gd–xZn alloys processed by equal channel angular pressing, *Mater. Sci. Eng. A*, 808(2021), art. No. 140921.

[146] A. Mohan, W. Yuan, and R.S. Mishra, High strain rate superplasticity in friction stir processed ultrafine grained Mg–Al–Zn alloys, *Mater. Sci. Eng. A*, 562(2013), p. 69.

[147] F. Chai, D.T. Zhang, Y.Y. Li, and W.W. Zhang, High strain rate superplasticity of a fine-grained AZ91 magnesium alloy prepared by submerged friction stir processing, *Mater. Sci. Eng. A*, 568(2013), p. 40.

[148] R.B. Figueiredo and T.G. Langdon, Strategies for achieving

high strain rate superplasticity in magnesium alloys processed by equal-channel angular pressing, *Scripta Mater.*, 61(2009), No. 1, p. 84.

[149] R. Motallebi, Z. Savaedi, and H. Mirzadeh, Post-processing heat treatment of lightweight magnesium alloys fabricated by additive manufacturing: A review, *J. Mater. Res. Technol.*, 20(2022), p. 1873.

[150] R. Motallebi, Z. Savaedi, and H. Mirzadeh, Additive manufacturing–A review of hot deformation behavior and constitutive modeling of flow stress, *Curr. Opin. Solid State Mater. Sci.*, 26(2022), No. 3, art. No. 100992.

[151] H. Khodashenas and H. Mirzadeh, Post-processing of additively manufactured high-entropy alloys - A review, *J. Mater. Res. Technol.*, 21(2022), p. 3795.

[152] K. Moeinfar, F. Khodabakhshi, S.F. Kashani-bozorg, M. Mohammadi, and A.P. Gerlich, A review on metallurgical aspects of laser additive manufacturing (LAM): Stainless steels, nickel superalloys, and titanium alloys, *J. Mater. Res. Technol.*, 16(2022), p. 1029.

[153] S. Rathee, M. Srivastava, P.M. Pandey, A. Mahawar, and S. Shukla, Metal additive manufacturing using friction stir engineering: A review on microstructural evolution, tooling and design strategies, *CIRP J. Manuf. Sci. Technol.*, 35(2021), p. 560.

[154] Y.H. Ho, K. Man, S.S. Joshi, *et al., In-vitro* biomineralization and biocompatibility of friction stir additively manufactured AZ31B magnesium alloy–hydroxyapatite composites, *Bioact. Mater.*, 5(2020), No. 4, p. 891.